CONFIDENTIAL

NACA

RESEARCH MEMORANDUM

EXPERIMENTAL INVESTIGATION OF DYNAMIC RELATIONS IN A 48-INCH RAM-JET ENGINE

By Herbert G. Hurrell

Lewis Flight Propulsion Laboratory
Cleveland, Ohio

NATIONAL ADVISORY COMMITTEE
FOR AERONAUTICS

WASHINGTON

February 15, 1957

CONFIDENTIAL

NACA RM E56F28

NATIONAL ADVISORY COMMITTEE FOR AERONAUTICS

RESEARCH MEMORANDUM

EXPERIMENTAL INVESTIGATION OF DYNAMIC RELATIONS IN A 48-INCH RAM-JET ENGINE

By Herbert G. Hurrell

SUMMARY

The dynamics of a large (48-in.) ram-jet engine were investigated for supercritical operation at a Mach number of 2.75 over a range of simulated altitudes from 68,000 to 82,000 feet. The investigation showed that the response of static or total pressure to fuel flow consisted of a dead time followed by a response form that, in general, approximated a linear, first-order, lead-lag. Dead time varied significantly only with distance from the combustion zone. Only slight differences in rise ratio and time constant existed for the various stations in the ram jet.

INTRODUCTION

The advent of the ram jet as a practical means of supersonic propulsion has necessitated the development of suitable controls for this type of engine. If any engine is to be precisely controlled, of course, the dynamics of that engine must be known. For the ram jet, however, very little dynamics information is currently available. Studies that contribute to the supply of such information are therefore greatly needed.

The many studies concerned with the dynamics of the turbojet engine do not aid greatly in determining the dynamics of the ram-jet engine. Entirely new problems in the dynamics field are presented by the ram jet, as well as by other systems whose thrust outputs are not dependent on the motion of mechanical components. With the turbojet, it was possible to neglect the dynamics of aerodynamic and thermodynamic processes because of the relatively slow dynamic behavior of the moving components. Such processes, however, are the sole contributors to the dynamics of the ram jet.

Experimental investigations have been conducted at the NACA Lewis laboratory to study the dynamic characteristics of the ram-jet engine. A 16-inch ram-jet engine designed for a Mach number of 1.89 was used in one test; and its dynamics were investigated in a supersonic wind tunnel over a range of Mach numbers, altitudes, and angles of attack. The results obtained are very briefly reported in reference 1. In another test, which was conducted in a free-jet facility, a 48-inch ram-jet engine designed for a Mach number of 2.75 was used; the dynamic relations in this engine are the subject of the present report. (Some preliminary results from the 48-in. engine are given in ref. 2.)

The dynamics of the 48-inch ram-jet engine were investigated by both indicial and frequency-response testing. The input variable was the engine fuel flow. The pressure response was recorded at several stations in the engine during transients that covered large ranges of engine operation in the supercritical region. The investigation was made at a Mach number of 2.75 and at zero angle of attack. Altitudes from 68,000 to 82,000 feet were simulated.

SYMBOLS

E	error voltage
G	Laplacian transfer function (pressure change to fuel-flow change)
K	steady-state gain
P	total pressure, lb/sq ft abs
p	static pressure, lb/sq ft abs
Δp_I	fuel orifice pressure drop for set of spray bars connected to servo system
Δp_{II}	fuel orifice pressure drop for set of spray bars connected to manual throttle
s	complex operator
V_i	fuel servo input voltage
V_f	fuel servo feedback voltage
w_f	fuel flow, lb/sec

Subscripts:

1 to 16 refer to pressures or pressure sensors located as shown in figs. 1(c) and 2(b)

APPARATUS AND INSTRUMENTATION

Engine

Diffuser. - A phantom sketch of the diffuser of the 48-inch ram-jet engine is shown in figure 1(a). The diffuser inlet was, essentially, a 216° segment of a single-cone (22° half-angle) Ferri type inlet. The conical shock wave fell just outside of the inlet lip at the Mach number of the investigation (2.75). The internal-flow passage of the diffuser was convergent-divergent; the area variation is shown in figure 1(b). In order to prevent flow separation, the diffuser included vortex generators placed along the cowl and innerbody. The performance of the diffuser is reported in reference 3.

For this investigation, a screen was installed near the diffuser exit across one-half of the flow passage to improve the velocity distribution at the diffuser exit. This screen blocked 20 percent of the half area.

The location of instrumentation in the diffuser is shown in figure 1(c). Twelve wall taps for the measurement of static pressures during transients were distributed longitudinally in the diffuser. Taps 1 to 11 were located on the top of the innerbody, 2 inches off-center, while tap 12 was located at 4:00 o'clock looking downstream. Two probes were used to measure total pressure during transients. Probe 14 was in the plane of the inlet lip at 12:00 o'clock. Probe 15 was at 2:00 o'clock near the diffuser exit. At each station where a pressure was measured during transients, the steady-state measurement of this pressure was made with a tap or probe in the close vicinity of the transient sensor. The average value of diffuser-exit total pressure over the cross section was determined from the pressures measured with the six rakes at station 196.5.

Combustor. - The ram-jet combustion chamber consisted of a 48-inch-diameter section $6\frac{1}{2}$ feet long connected to the 32-inch-diameter diffuser outlet by a 30° (included-angle) divergent section. The fuel injection system and a portion of the flameholders were contained in this divergent section. A cutaway view of the combustor is shown in figure 2(a), and a diagramatic sketch is shown in figure 2(b).

Fuel was sprayed normal to the air stream through orifices in 1/2-inch-diameter radial bars. The combustor contained three sets of spray bars; a set consisted of 16 bars equally spaced circumferentially and supplied from a common external manifold. Figure 2 shows the three bars present at a typical circumferential position; however, only the two upstream sets of spray bars were used in this investigation.

The fuel used was MIL-F-5624B, grade JP-5, with a lower heating value of 18,625 Btu per pound.

Information on combustor performance and further details of combustor design are contained in reference 4.

Exhaust nozzle. - The convergent-divergent exhaust nozzle is also shown in figure 2(b). The throat area of the nozzle was 54.6 percent of the maximum area of the combustion chamber.

The nozzle inlet was instrumented as shown in figure 2(b). Transient measurements were made with total-pressure probe 16 and wall static tap 13. The rakes were used to determine the average value of total pressure over the cross section in steady state.

Facility

The investigation was conducted in a free-jet facility. The design and performance of this facility are discussed in reference 5. Figures 3(a) and (b) show a schematic diagram and a cutaway view, respectively, of the facility with the ram-jet engine installed. The inlet of the supersonic nozzle was supplied with dried and heated compressed air. About 52 percent of the free jet from the supersonic nozzle entered the engine inlet; the remainder passed through the jet diffuser. The combined flow from the ram jet and the jet diffuser was ducted to exhausting machinery.

Fuel System

As mentioned previously, two sets of fuel spray bars were used in the investigation. The fuel flow to the downstream set was controlled manually and was not varied during transients. The fuel flow to the upstream set was controlled by a specially designed fuel system and was used to impose transient operation on the engine.

The block diagram of this fuel system is shown in figure 4. The system consisted of a throttle with a pressure-drop control and a closed-loop servo system for positioning the throttle. The throttle-pressure-drop control maintained a constant pressure differential across the

throttle by means of a fast-acting pressure-reducing valve. The flow through the throttle, therefore, varied linearly with throttle position (throttle area was proportional to position). The electrohydraulic servo system provided a linear relation between throttle position and the input voltage V_i. Fuel flow, therefore, was a linear function of the input voltage. Further details on the design of fuel systems of this type are given in reference 6.

The dynamic performance of the fuel system, as installed for the investigation, is shown in figure 5. In this figure is shown the frequency response of fuel-throttle position to servo input voltage, fuel flow (at the spray orifices) to servo input voltage, and fuel flow to fuel-throttle position. The data involving fuel flow include the dynamic effects of the manifold on the engine and all the necessary piping leading to the manifold. (The fuel system shown in fig. 4 was mounted outside the free-jet facility.) The performance of the system makes it suitable for the investigation of ram-jet dynamics.

4092

Instrumentation

Gas-pressure sensors. - Pressure pickups of the variable-inductance type having high natural frequencies were used to measure gas pressures in transient. The pickups were very small and of diaphragm construction. They were installed in water-cooled jackets to maintain operation at the high temperatures involved. Connecting tubing lengths were kept to a minimum to ensure fast response; all pickups had tubing lengths of 9 inches, except pickups 15 and 16, which had lengths of 9.5 and 23.75 inches, respectively. In order to give satisfactory damping, tubing with an inside diameter of 0.040 inch was used.

The response characteristics of the pickups without tubing and with two different lengths of tubing were obtained from bench tests and are presented in figure 6. The figure shows that tubing length affected the response mainly in the frequency range over 100 cycles per second. With 9 inches of tubing, the response was nearly flat at frequencies up to 100 cycles per second.

For steady-state measurements, pressures were indicated on manometers and recorded simultaneously by photography.

Fuel flow. - An indication of the fuel flow from each set of spray bars during transients was obtained by measuring the pressure drop across the orifices in the spray bars. A resistance, strain-gage, differential-pressure pickup was connected to the line between a spray bar and its manifold and was referenced to the gas pressure in the combustion chamber near the spray bars. Bench tests showed the response of the fuel-pressure side of the pickups (with the tubing involved) to be essentially flat to 150 cycles per second with no measurable phase shift.

[redacted]

Steady-state measurements of fuel flow were made with manometers which indicated the pressure drop across an orifice in the fuel supply line to the facility.

Fuel-throttle position. - Fuel-throttle position was sensed by a linearly variable differential transformer directly attached to the throttle. The signal was amplified, demodulated, and filtered giving a direct-current signal proportional to the throttle position.

Amplifiers and recorders. - Carrier-type amplifiers were used for the pressure signals. The voltage indicative of fuel-throttle position and the fuel servo input voltage were amplified by direct-current amplifiers. The carrier amplifiers are shown in racks 1 and 3 of figure 7 and the direct-current amplifiers in rack 5.

The transient measurements were recorded on sensitized paper with oscillographs using galvanometers with natural frequencies of 210 to 500 cycles per second, depending on the amount of filtering desired. For monitoring purposes, certain variables were also recorded with a direct-inking strip-chart recorder.

The galvanometric oscillographs are shown in racks 2 and 4 of figure 7 and the direct-inking recorder in rack 7.

PROCEDURE

The investigation was conducted at a Mach number of 2.75, zero angle of attack, and over a range of simulated altitudes from 68,000 to 82,000 feet. The total temperature of the inlet flow to the ram jet was maintained close to 528° F, the temperature value corresponding to flight above the tropopause at this Mach number.

The desired flow conditions in the free jet could not be maintained when the ram jet was operated subcritically. The tests, therefore, were limited to the supercritical operating region of the engine. The steady-state map of this region is presented in figure 8, where diffuser total-pressure recovery is shown as a function of fuel-air ratio. Only a limited amount of data was obtained close to the critical point (approximately 0.63 recovery) because of the delay involved in reestablishing the free-jet flow after a flow breakdown. A substantial portion of the map shown was covered in the indicial and frequency-response tests of the engine dynamics.

Indicial response was investigated by the addition of a step function to the input voltage of the fuel servo. The resulting disturbance in fuel flow approximated a step; the rise time was about 0.010 second in most cases. This was considered an adequate step for the purposes

of this investigation and will be referred to as a step in fuel flow. Both step increases and decreases in fuel flow were made from several initial levels. These initial levels in fuel flow were chosen to cover the range of engine operation given in figure 8. Steps of various magnitudes from fixed levels were also made. The magnitudes of the steps were varied from 10 to 38 percent of the fuel flow required for critical operation of the ram jet. Steady-state data were taken to determine the initial and final conditions of each transient.

4092

Frequency response was investigated by imposing a sinusoidal variation on the input voltage of the fuel servo. The form of the resultant variation in fuel flow was essentially sinusoidal over the frequency range of interest. The mean value and the amplitude of each fuel-flow sinusoid were held constant while recordings were made for several discrete frequencies. At the higher frequencies, it was necessary to increase the amplitude of the voltage sine wave in order to maintain a constant fuel-flow amplitude (see fig. 5). The frequency range was also swept while continuous recordings were made in order to discover any phenomena that might be isolated in a narrow frequency band. Steady-state data corresponding to the peaks and mean value of each sine wave were recorded. The engine was subjected to sinusoidal variations in fuel flow of various amplitudes and mean values selected to cover a large portion of the supercritical operating region. Frequency-response data are presented for frequencies up to 50 cycles per second.

RESULTS AND DISCUSSION

General Characteristics of Response

An orderly approach to the determination of engine dynamics is first to investigate transients sufficiently small to involve only dynamic relations that are essentially linear and then to investigate the nonlinear effects that may arise during larger transients. In this investigation, however, it was necessary to use rather large fuel-flow transients in order to provide transients in the engine pressures that were discernible over the noise levels present. The results, therefore, are not entirely free of the nonlinear effects of the unsteady-flow processes involved. In spite of this, the responses obtained generally approximated a linear form within a reasonable degree of accuracy. In general, the response of pressure to fuel flow consisted of a dead time followed by a first-order lead-lag. This manner of response is also noted in the investigation reported in reference 1.

In the present investigation, departures from the linear lead-lag pattern were observed in particular cases. These departures, however, occurred when the transient included operating regions where nonlinearities existed in the static relation of particular pressures to fuel flow. Such nonlinearities were caused by the proximity of the shock wave or by transverse distortions in the flow.

A detailed presentation of the results obtained from the indicial- and frequency-response testing will be given in following sections. In the remainder of this section, typical responses will be discussed in order to introduce the various phenomena involved in the later discussions.

Transient records of a typical response to a step increase in fuel flow are shown in figure 9. Two records are shown because the large number of pressures necessitated the use of two recorders. The trace at the top of each record is a synchronizing trace, which permits the time scales of the two records to be correlated. In addition, correlation is possible by means of the step in fuel servo input voltage V_i which appears in both records. The transient presented in the figure resulted from a fuel-flow step of about 32 percent of the critical fuel flow at the simulated altitude of 82,000 feet. The approximate movement of the diffuser normal shock during the transient was from station 135 (p_9) to station 45 (p_4).

The dead time in the pressure response is apparent in figure 9. This dead time is the time interval from a fuel-flow change (Δp_I trace) to the beginning of a pressure response. A dead time of 0.021 second, for example, can be read from the trace of p_{13}. The dead time consisted of two delays: the first was the time expired between an increase in fuel flow at the injection station and the increase in heat release at the combustion zone, and the second was the time required for the resultant pressure disturbance to propagate from the combustion zone to the pressure sensor. If the dead times in figure 9 for diffuser static pressures are read in succession from the exit (p_{12} to p_5), it will be seen that they become progressively larger, marking the upstream propagation of the pressure disturbance.

The disturbance, of course, propagated against the relatively low velocities of subsonic flow to the initial position of the shock (p_9). Further propagation upstream (p_9 to p_4) had to be accomplished by shock movement against supersonic air velocities and, consequently, was at a slower rate. Dead times at the stations passed by the shock were not, therefore, representative of the dead times at these stations when the shock was initially upstream of them. In order to distinguish the dead times according to the manner of propagation involved, the term

dead time will be used herein only when the pressure was sensed downstream of the initial shock position. The dead time of pressures upstream of the initial shock position will be called "shock-passage time." As an example, a shock-passage time of 0.078 second is noted in figure 9 for p_7. The shock-passage time of a given station consists of the dead time at the initial shock position plus the time required for the shock to travel to the given station.

The controlled pressure in a ram-jet control system, of course, will not be sensed upstream of the steady-state shock position, except in the special case of limiting controls. Shock-passage time, therefore, need not be considered in the study of stability and response to small disturbances; however, it may be an important part of the control problem when large disturbances are involved. Knowledge of shock-passage times is useful also in determining how fast a control must respond if it is necessary to keep the shock within the diffuser, that is, to avoid subcritical operation of the engine.

Also illustrated in figure 9 is the lead-lag form, characteristic, in general, of the pressure response. This manner of response, in which the pressure responds directly proportional to fuel flow at first and then approaches its final value in exponential manner, is most apparent in the traces of p_{10} and p_{11}. The lead-lag is also present in the traces of p_{12}, p_{13}, and p_{16} but is somewhat obscured by the noise level. For p_{15}, the exact nature of response is completely hidden in this record by the noise. Pressure response upstream of p_{10} was dependent on the configuration and speed of the shock as it passed a particular station.

Transient records of a typical response to a step decrease in fuel flow are shown in figure 10. This was the return transient of that shown in the preceding figure, that is, the step decrease in fuel flow (32 percent of the critical value) was made from the steady-state conditions that followed the transient of figure 9. Because the initial shock position for the transient of figure 10 was near station 45 (p_4), the normal dead times of pressures as far upstream as p_5 can be read from this figure. The dead time of p_7 (0.041 sec) is noted in the figure for comparison with the shock-passage time (0.078 sec) shown in the previous figure for this pressure. Downstream of the region of shock travel, the dead times in the two figures are about the same for a given pressure. For static pressures p_{10} to p_{13}, which were downstream of the shock travel, the response after dead time appears to approximate the lead-lag form. The general response form of pressures further upstream is not apparent in this figure because the passing of the shock interfered with the pressure responses.

As stated previously, the remaining sections of the report contain a more detailed presentation of the response characteristics already introduced. Data from the indicial-response tests are used in presenting information on dead time and shock-passage time. The results of the frequency-response tests are used to establish the form of response and the transfer functions.

Dead Time

The data given in this section are for static pressures only since the traces of total pressures were too noisy to read accurately in the indicial-response records. Frequency-response data, however, showed the dead time of total pressure to be about equal to the dead time of static pressure at a given station. These frequency-response data will be presented in the section "Response of total pressures."

Variation with ram-jet station. - The variation of dead time with ram-jet station is shown in figure 11. This figure shows the dead times resulting from a step decrease in fuel flow equal to 10 percent of the critical fuel flow at the simulated altitude of 82,000 feet. The step was taken from a high diffuser total-pressure recovery (0.616) in order to obtain data for stations as far upstream as possible. Although this recovery was about 98 percent of critical recovery, the shock position was considerably downstream of the diffuser inlet because of the internal contraction and slow initial divergence of the flow passage. No dead-time data, therefore, could be obtained for pressures p_1 to p_4. (As discussed previously, the subcritical region had to be avoided because of the facility limitation.)

As shown in figure 11, dead time varies from 0.019 second for the exhaust-nozzle inlet (p_{13}) to 0.052 second for the farthest upstream measurement (p_5). Considering only the variation within the diffuser (diffuser pressures are most suited for control purposes), the dead time of p_5 is more than twice the dead time near the diffuser exit (p_{12}). This appreciable increase in dead time with distance from the combustion zone is a significant factor to consider when selecting the sensor location for a control that will manipulate fuel flow. A sensor located near the diffuser exit would allow faster response for a high-recovery control than would a sensor located near the steady-state shock position, that is, if the other factors affecting response are equal.

Effect of diffuser recovery and step direction. - The effect of diffuser total-pressure recovery and the direction of the fuel-flow step on dead time is presented in figure 12. In this figure the dead times for several pressures are shown as functions of diffuser recovery for both step increases and decreases in fuel flow. The magnitude of the

steps was again 10 percent of the critical fuel flow, and the simulated altitude was still 82,000 feet. Data are shown only for pressures p_9 to p_{13} because the other static pressures were not downstream of the shock for a sufficient range of recoveries.

Figure 12 shows that the dead times were not dependent on whether the step was an increase or a decrease in fuel flow.

Pressures relatively near the combustion zone (p_{11} to p_{13}) have no apparent variation in dead time with diffuser total-pressure recovery (fig. 12). For pressures farther upstream (p_9 and p_{10}), however, a slight decrease in dead time with increasing pressure recovery is noticeable. This decrease resulted because the air velocities opposing the upstream propagation of the pressure disturbance were reduced by an increase in pressure recovery. The time required for the propagation of the pressure disturbance was, of course, a more significant portion of the dead time for the upstream pressures than for the downstream pressures.

Effect of step magnitude. - No variation in dead time with the magnitude of the fuel-flow steps was observed. Steps were investigated that ranged in magnitude from 10 to 38 percent of the critical fuel flow at the simulated altitude of 82,000 feet. The data for step decreases in fuel flow over this range of magnitudes are shown in figure 13(a) for a pressure well forward in the diffuser p_5 and for a pressure near the diffuser exit p_{12}. These data were taken at a high initial value of diffuser recovery (0.615). With step increases in fuel flow, it was necessary that the initial recovery be low (0.531) in order to avoid entering the subcritical region in the transients; hence, the initial shock position was well downstream and data were not obtained for pressures very far forward in the diffuser. Figure 13(b) shows the data obtained for p_{12} from the step increases in fuel flow.

Effect of altitude. - Figure 14 shows that dead time does not vary with altitude over the range that was simulated (68,000 to 82,000 ft). The dead times shown in the figure are for step increases in fuel flow taken from initial recoveries of 0.592. The magnitudes of the steps were such that a change in fuel-air ratio of 0.006 was made at each altitude.

Shock-Passage Time

Because it was not expedient to expel the shock during the investigation, the information obtained on shock-passage time was rather limited. Some information, however, is given by the data shown in figure 15. This figure shows the variation of shock-passage time with

ram-jet station for step increases in fuel flow of various magnitudes. The initial diffuser total-pressure recoveries and, hence, initial shock positions were the same for all the steps. The steps were taken at a simulated altitude of 82,000 feet.

In order to illustrate the large difference between shock-passage time and the normal dead time, the dead-time curve from figure 11 is also shown in figure 15. A comparison of the slopes of the curves shows that the shock travelled at rates which were much slower than those for a disturbance propagating through the same portion of the diffuser against subsonic flow.

The shock-passage times shown in figure 15 decrease at a given station as the magnitude of the fuel flow step is increased. The average speed at which the shock moved upstream from its initial position became faster, therefore, as the disturbances were made larger.

Response Form and Transfer Functions

The form of response and the transfer functions, as stated previously, were determined from the frequency-response data. These data are presented for a simulated altitude of 68,000 feet only; however, the response did not change significantly with altitude over the range simulated during the investigation (68,000 to 82,000 ft).

Static characteristics. - Three sinusoidal variations in fuel flow were used to obtain the frequency-response data presented. The steady-state operating regions corresponding to these sinusoids are indicated in figure 16(a), which shows the fuel-flow range of each sinusoid in relation to the steady-state variation of diffuser total-pressure recovery with fuel flow. It is apparent from this figure that a wide range of engine operation was covered in the frequency-response tests. The figure also shows that sinusoids A and B, considered together, provide a change in amplitude at constant base point, while sinusoids B and C provide a change in base point at constant amplitude.

The steady-state relations of the individual pressures to fuel flow are presented in figures 16(b) (static pressures) and (c) (total pressures). (Data are not shown for p_{13}, because the installation of this pickup proved unsuitable for frequency-response testing.) For convenience, the fuel flows covered by each sinusoid are indicated again on these figures. The figures show that some of the pressures were reasonably linear in their static relation to fuel flow, while others were very nonlinear.

The shock wave was responsible for the principal nonlinearities in the static pressures. For the lowest value of fuel flow for which the data of figure 16(b) are shown, the shock was just upstream of the station where p_9 was measured. As the fuel flow was increased over the range used to acquire the data, the shock moved past the stations of p_8, p_7, p_6, and p_5, resulting in the very nonlinear behavior of these pressures. The static pressures at stations not passed by the shock (p_9, p_{10}, p_{11}, and p_{12}) varied in a reasonably linear manner. (The proximity of the shock to the station of p_9 did affect this pressure somewhat for the lower values of fuel flow, but for the larger portion of the range the behavior of p_9 was reasonably linear.)

The curve for total pressure P_{15} (fig. 16(c)) shows the steady-state variation of this pressure was also quite nonlinear. This was a result of the changes that occurred in the transverse flow distortions of the diffuser when the fuel flow was varied. These changes were evident on examining the total-pressure surveys taken with the six rakes at this station. (It is interesting to compare the curve for P_{15} with the relatively linear curve of fig. 16(a), which indicates the behavior of the cross-sectional average pressure with fuel flow.)

Response of static pressures. - On the basis of the steady-state relations given in figure 16(b), nonlinearities attributable to the shock were to be expected in some of the static-pressure responses. Where such nonlinearities were not involved, however, the responses of the static pressures approximated a linear form.

Several of the static pressures (p_9, p_{10}, p_{11}, and p_{12}) were downstream of the region of shock travel during all three of the sinusoids. The frequency response of these pressures to fuel flow is presented in figure 17, where amplitude ratio and phase lag are shown as functions of frequency for each of the pressures. The amplitude ratios are given in normalized form; that is, they have been divided by the amplitude ratios at frequencies sufficiently low to represent steady state. Curves representing the amplitude ratio and phase lag of a linear, first-order, lead-lag function (with dead time) have been fitted to the data for each pressure. The Laplacian transfer functions associated with the curves are also given in the figure. (Numerical values for the steady-state gain terms, which are shown symbolically in the transfer functions, can be determined from the curves of fig. 16(b).)

Figure 17 shows that, for each pressure of this group, the responses to all three sinusoids can be represented by the same transfer function with a reasonable degree of accuracy. Minor variations with amplitude or base point, though, are apparent for a given pressure. (For example,

the data for p_9 from sinusoids A and B show a small-amplitude effect.) Such variations, however, show no regular trends from one station to another and are small in comparison with the predominant response form.

An inspection of the transfer functions in figure 17 will show that the variations in rise ratio and time constant between the various pressures are small. Rise ratios vary from 0.47 to 0.56, and time constants vary from 0.080 to 0.091 second.

The terms for dead time that were required in the transfer functions in order to match the phase-lag curves with the data agree very well with the values of dead time obtained from the indicial-response tests. This agreement can be seen by comparing the exponential terms in the transfer functions of figure 17 with the values of dead time shown in figure 12. For example, dead times of 0.020 and 0.021 second are indicated for p_{12} in figures 17 and 12, respectively.

For the remaining static pressures (p_5, p_6, p_7, and p_8), nonlinearities caused by the shock occurred within the fuel-flow range covered in the frequency-response tests. These pressures were sensed at stations far enough upstream to be passed by the shock during sinusoids A and B. When the shock moved downstream of a tap, of course, the flow past the tap became supersonic and the pressure no longer responded to the varying fuel flow. This phenomenon appeared in the transient record as a clipping of the sine wave traced by the pressure. For sinusoid C, some of the wave forms were quite distorted from a true sine wave, even though the flow did not become supersonic at the stations involved. The pressure effects of the shock, of course, extended some distance into the subsonic region.

The curves in figure 16(b), however, show that one pressure in this group p_6 varies in a nearly linear manner over the fuel-flow range of sinusoid C, at least in steady state. The frequency response of this pressure for this range of fuel flows is shown in figure 18. In addition to the data from sinusoid C, data are shown from sinusoid A for the portion of the sine wave corresponding to subsonic flow past the pressure tap. (The traces for sinusoid C, however, permitted a more accurate determination of the data points.) Figure 18 shows that, over the fuel-flow range involved, the dynamic response of p_6 is essentially linear and, like the responses already presented, can be adequately described as a lead-lag with dead time. Both the rise ratio (0.50) and the time constant (0.080 sec) are very similar to the values presented for other static pressures. The dead time indicated by the phase-lag data in figure 18 (0.043 sec) is the same as that obtained in the indicial-response tests (fig. 11).

For each of the remaining static pressures (p_5, p_7, and p_8), there were certain limited regions of fuel flow where the steady-state relation was nearly linear (fig. 16(b)). On the basis of the response determined for p_6, it is believed that, in these particular regions of fuel flow, these pressures would also respond in linear lead-lag fashion (following dead time).

Response of total pressures. - The frequency responses of total pressures P_{15} and P_{16} are presented in figure 19. (Total pressure P_{14} was always upstream of the shock and did not respond.) Figure 19(a) shows that the response of P_{16} approximates a single lead-lag function (with dead time) for all three sinusoids. The data that are shown in figure 19(b) for P_{15} also indicate the same type of response. The data for P_{15}, however, are shown just for sinusoid B, and only frequencies to 10 cycles per second are included for this sinusoid. For sinusoids A and C, and for the higher frequencies of sinusoid B, P_{15} did not respond in linear fashion. As previously shown (fig. 16(c)), P_{15} was considerably nonlinear in its relation to fuel flow in steady state; this nonlinearity was attributed to the changing flow distortions of the diffuser. On the basis of the steady-state curve, it appeared that this problem would be associated mainly with high fuel flows and thus only with sinusoids A and C. At the higher frequencies, however, the distortion problem was evidently extended to the fuel-flow range of sinusoid B.

The rise ratios and the time constants obtained for total pressures (fig. 19) are very similar to those obtained for static pressures. The rise ratios that are presented for static pressures vary from 0.47 to 0.56. A value within this range (0.50) was obtained for P_{15}, while the value for P_{16} (0.44) was just a small amount outside this range. The time constants presented for static pressures vary from 0.080 to 0.091 second. The time constants for P_{15} (0.086 sec) and P_{16} (0.089 sec) are both within this range.

As mentioned previously, the phase-lag data gave the best indication of total-pressure dead time because the high noise level of these pressures made the step data difficult to read. The phase-lag curves in figure 19 indicate that the dead times of P_{15} and P_{16} are 0.022 and 0.018 second, respectively. A comparison of these values with the dead times presented earlier for p_{11} (0.022 sec) and p_{13} (0.019 sec) indicates that the dead times of total and static pressure are about equal at a given station.

SUMMARY OF RESULTS

Dynamic relations in a large (48-in.) ram-jet engine have been experimentally investigated for a range of supercritical operating points and for a range of flight conditions (Mach number, 2.75; angle of attack, zero; simulated altitudes, 68,000 to 82,000 ft). The results of the investigation can be summarized as follows:

1. Throughout the ram-jet engine, and for transients covering a wide range of supercritical operation, the response of static or total pressure to fuel flow consisted of dead time followed by a response form that, in general, approximated a linear, first-order, lead-lag.

2. Any significant departures from the lead-lag form were explainable on the basis of nonlinearities that were caused by the shock or by transverse distortions in the flow.

3. The rise ratios and time constants determined for static and total pressures were nearly independent of ram-jet station. Rise ratios varied from 0.44 to 0.56; time constants, from 0.080 to 0.091 second.

4. At a given station, the dead times of static and total pressures were about equal.

5. For stations downstream of the shock, the dead times varied significantly only with distance from the combustion zone. These dead times ranged from 0.019 second at the exhaust-nozzle inlet to 0.052 second near the diffuser inlet and did not vary with the direction of the fuel-flow step, the magnitude of the step, or the simulated altitude. There was a slight decrease in dead time with increasing diffuser total-pressure recovery for pressures sensed a considerable distance from the combustion zone.

6. The dead time at a given station to a step increase in fuel flow became much greater when the shock was initially downstream of that station. In other words, shock travel was much slower than the propagation of a disturbance against subsonic flow. Shock travel became faster as the magnitude of the step was increased.

Lewis Flight Propulsion Laboratory
National Advisory Committee for Aeronautics
Cleveland, Ohio, July 20, 1956

REFERENCES

1. Vasu, G., Wilcox, F. A., and Himmel, S. C.: Preliminary Report of Experimental Investigation of Ram-Jet Controls and Engine Dynamics. NACA RM E54H10, 1954.

2. Vasu, George, Hart, Clint E., and Dunbar, William R.: Preliminary Report on Experimental Investigation of Engine Dynamics and Controls for a 48-Inch Ram-Jet Engine. NACA RM E55J12, 1956.

3. Farley, John M., and Seashore, Ferris L.: Full-Scale, Free-Jet Investigation of Methods of Improving Outlet Flow Distribution in a Side-Inlet Supersonic Diffuser. NACA RM E54L31a, 1955.

4. Rayle, Warren D., Smith, Ivan D., and Wentworth, Carl B.: Preliminary Results from Free-Jet Tests of a 48-Inch-Diameter Ram-Jet Combustor with an Annular-Piloted Baffle-Type Flameholder. NACA RM E54K15, 1955.

5. Seashore, Ferris L., and Hurrell, Herbert G.: Starting and Performance Characteristics of a Large Asymmetric Supersonic Free-Jet Facility. NACA RM E54A19, 1954.

6. Otto, Edward W., Gold, Harold, and Hiller, Kirby W.: Design and Performance of Throttle-Type Fuel Controls for Engine Dynamic Studies. NACA TN 3445, 1955.

[redacted]

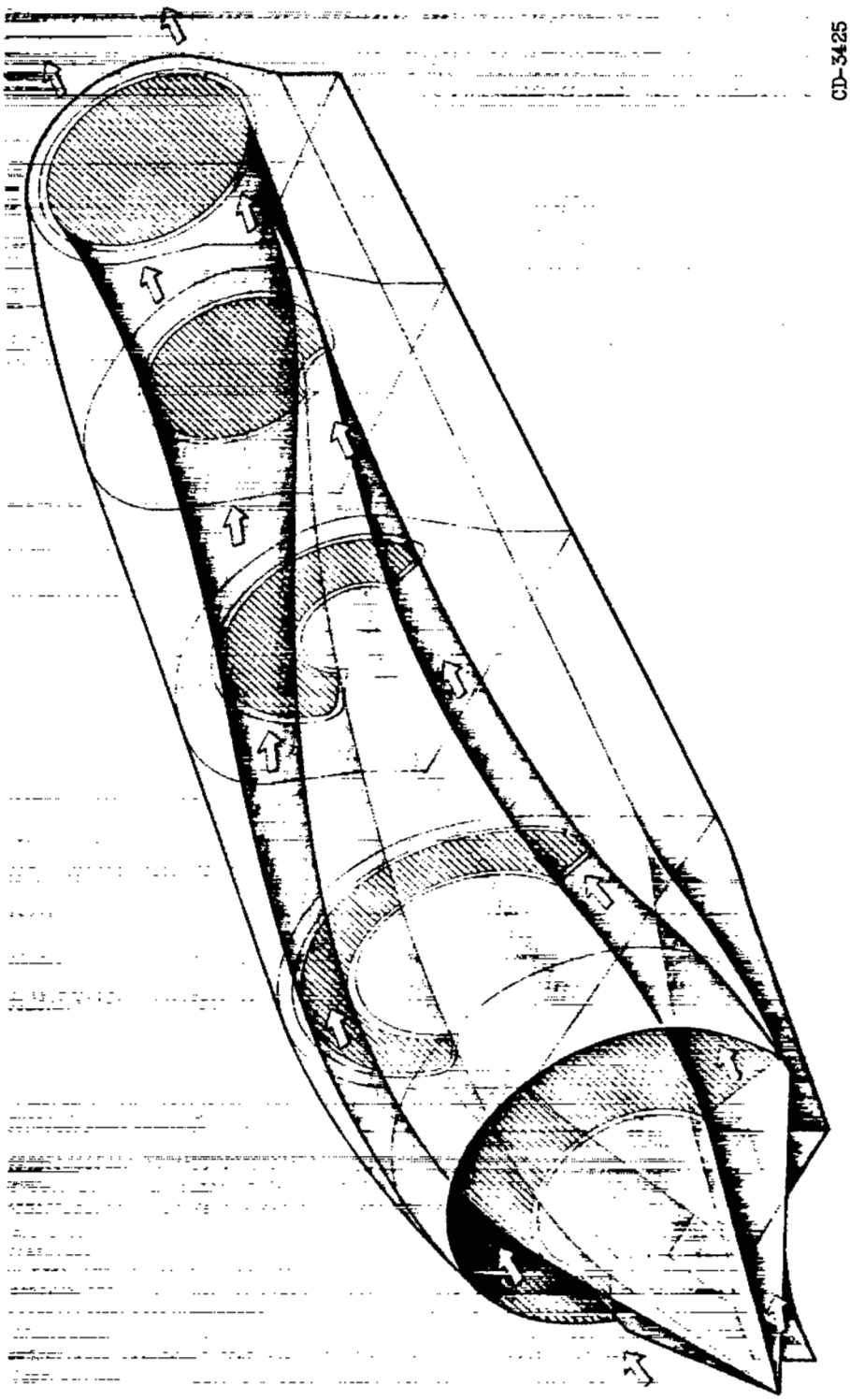

(a) Isometric view.

Figure 1. - Ram-jet diffuser.

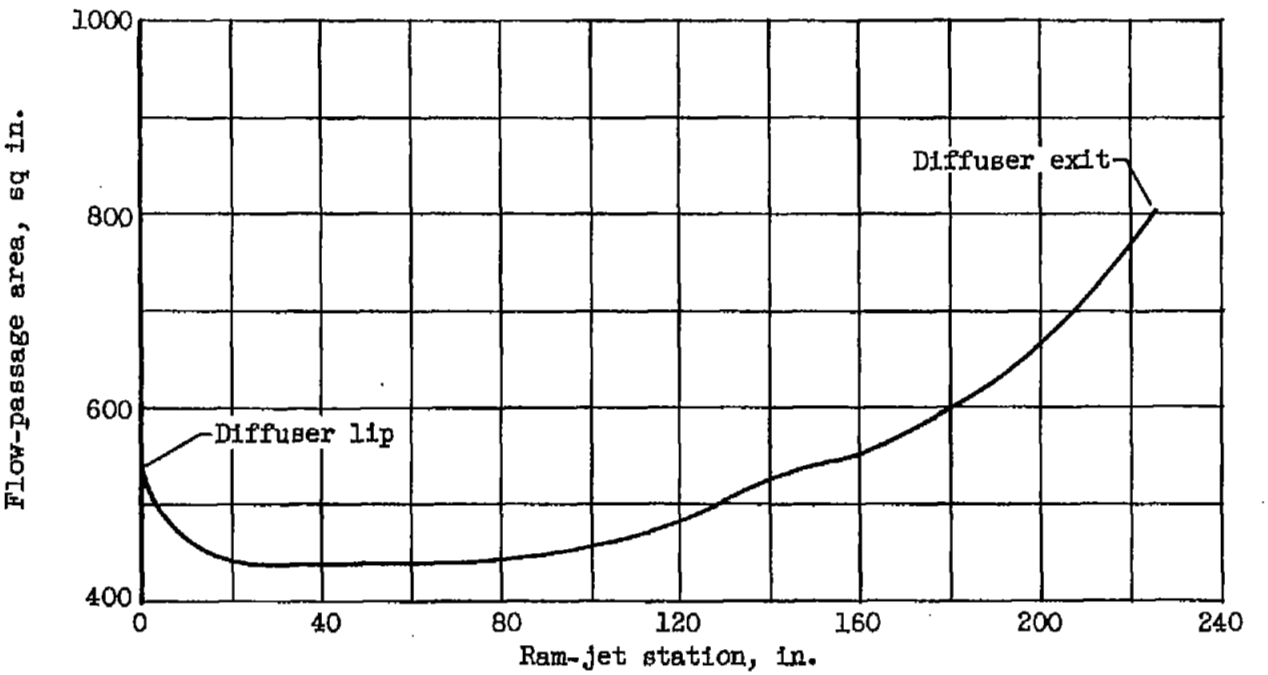

(b) Area variation.

Figure 1. - Continued. Ram-jet diffuser.

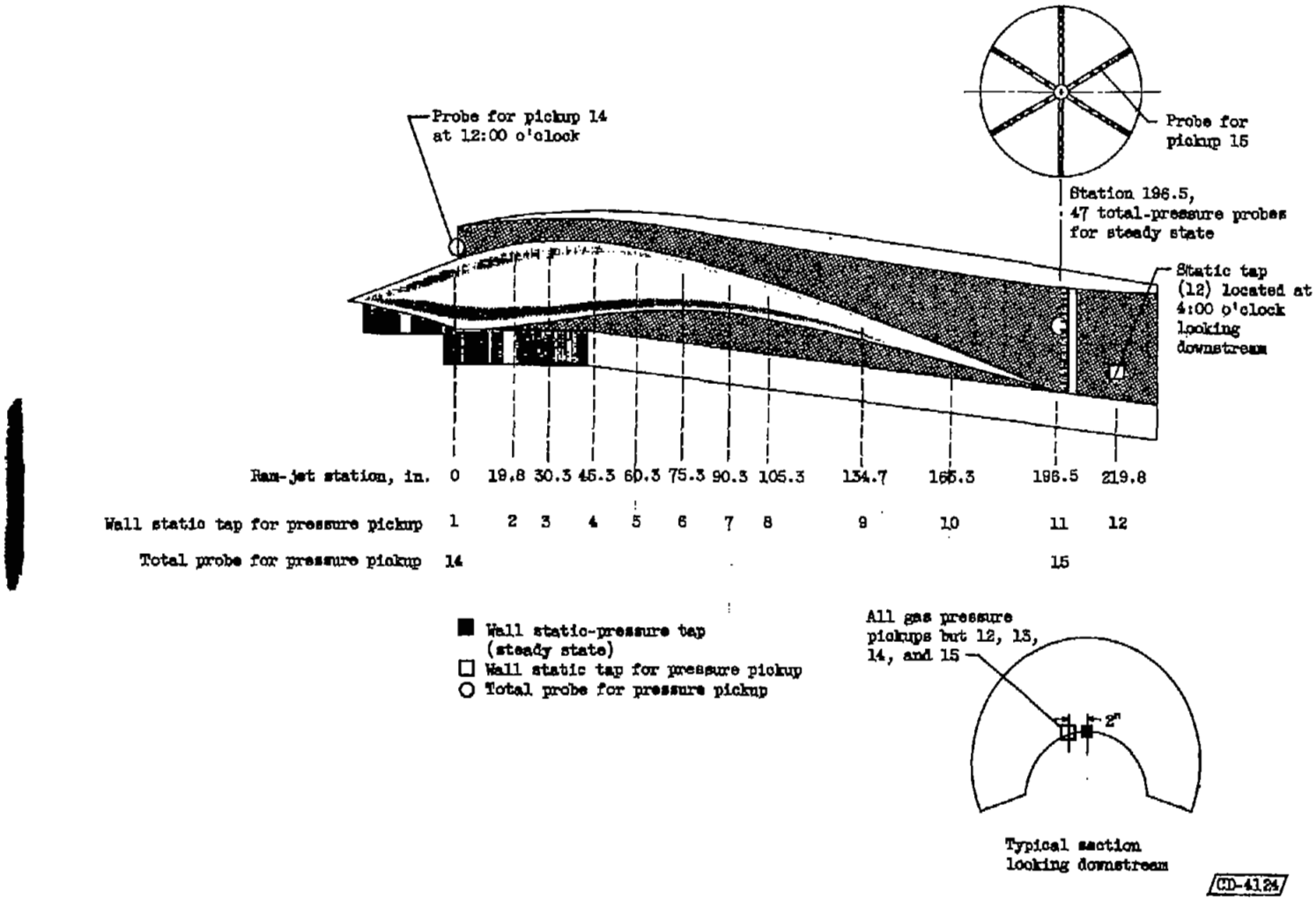

(c) Location of instrumentation.

Figure 1. - Concluded. Ram-jet diffuser.

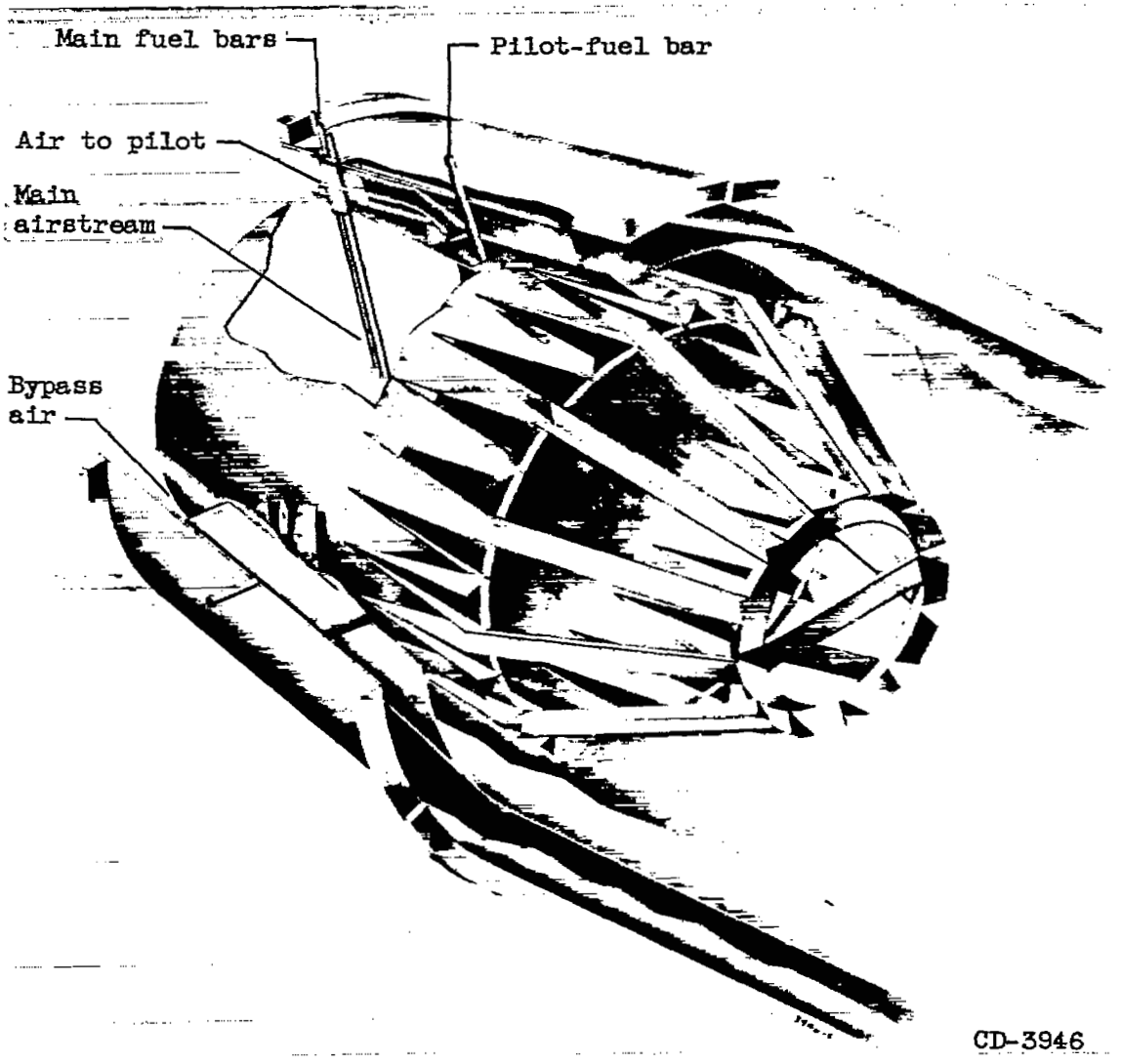

(a) Cutaway view.

Figure 2. - 48-Inch ram-jet combustor.

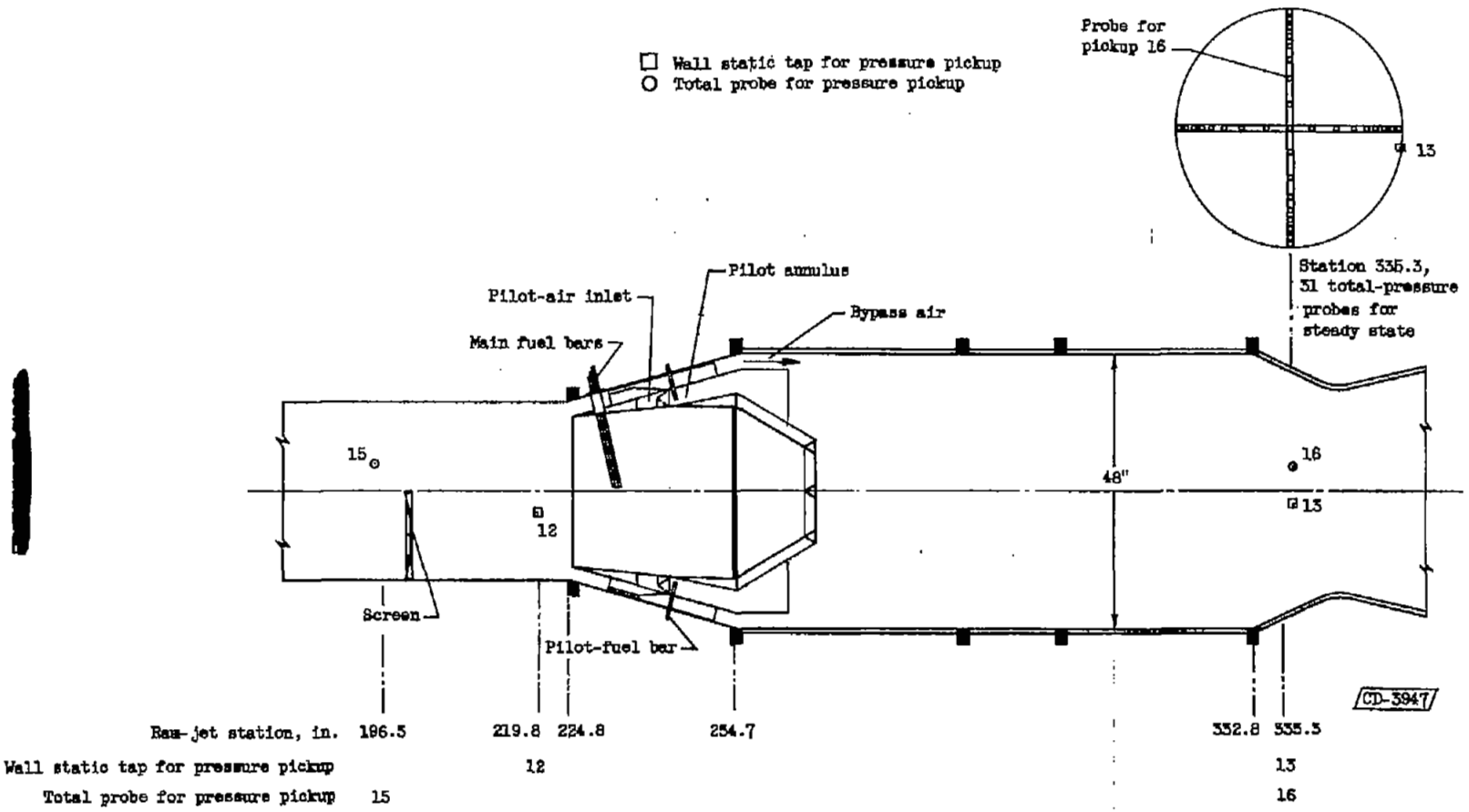

(b) Location of instrumentation.

Figure 2. - Concluded. 48-Inch ram-jet combustor.

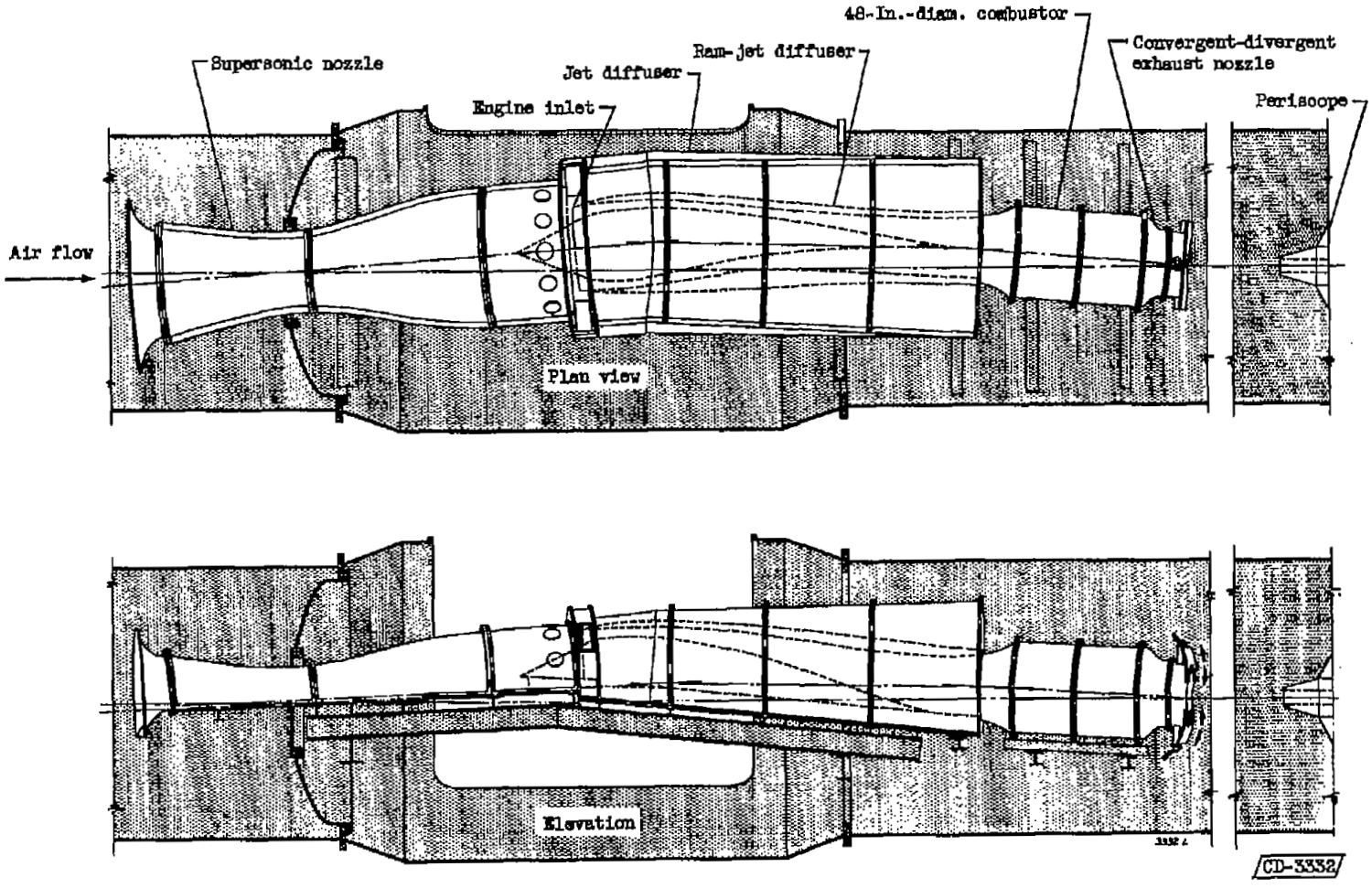

(a) Schematic diagram.

Figure 3. - Free-jet installation of 48-inch ram-jet engine.

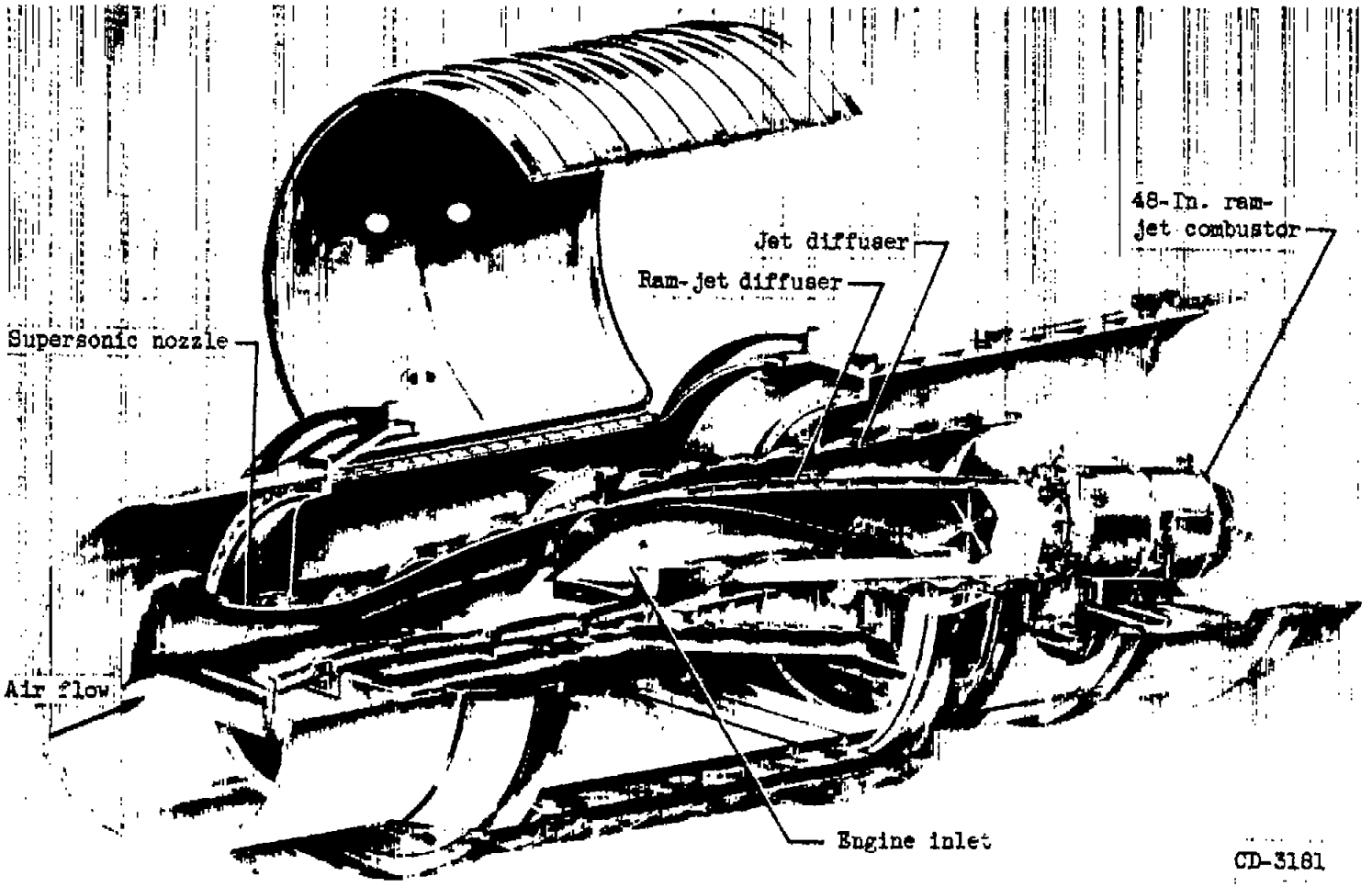

(b) Cutaway view.

Figure 3. - Concluded. Free-jet installation of 48-inch ram-jet engine.

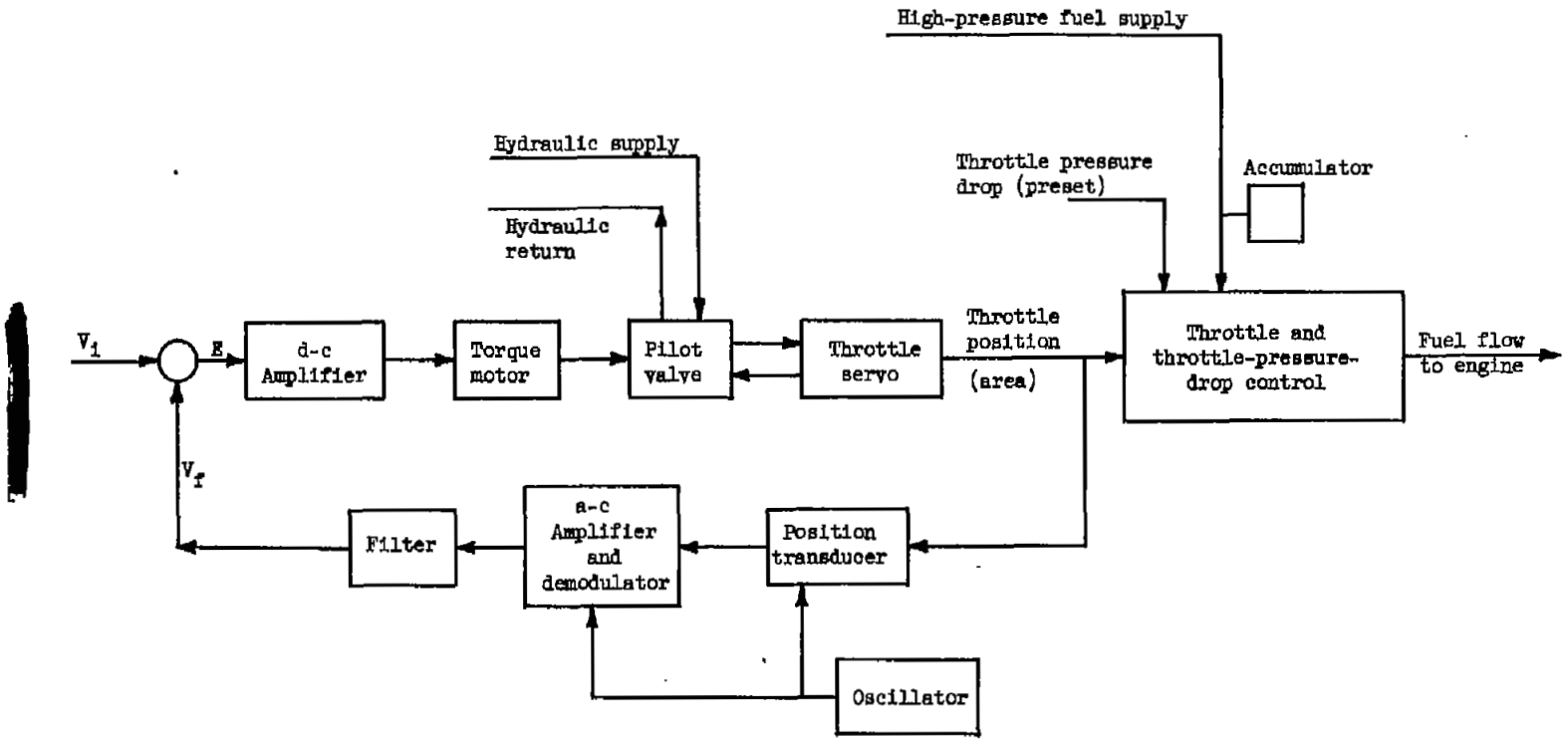

Figure 4. - Block diagram of fuel system used for engine dynamics investigation.

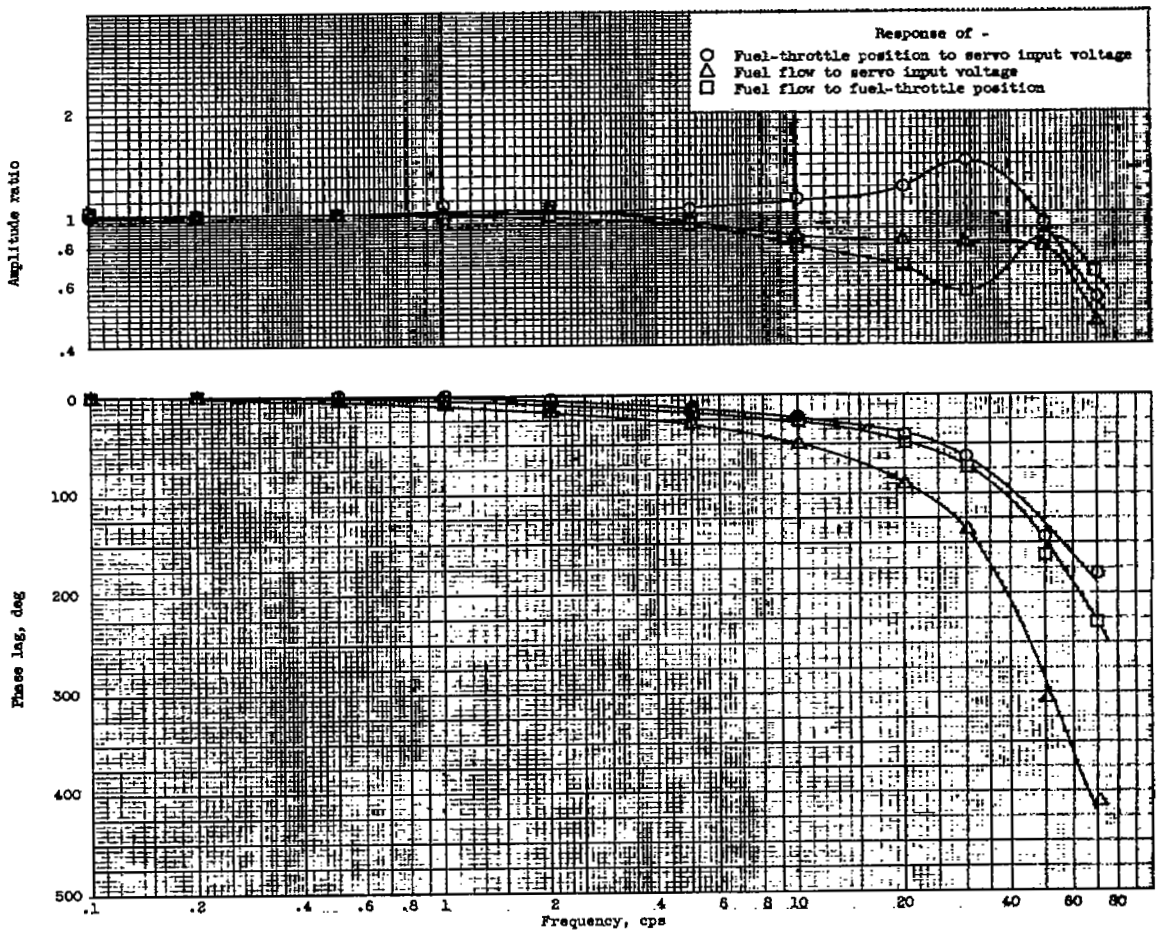

Figure 5. - Frequency response of fuel system. Base fuel flow, 1.68 pounds per second; fuel-flow amplitude, 0.403 pound per second.

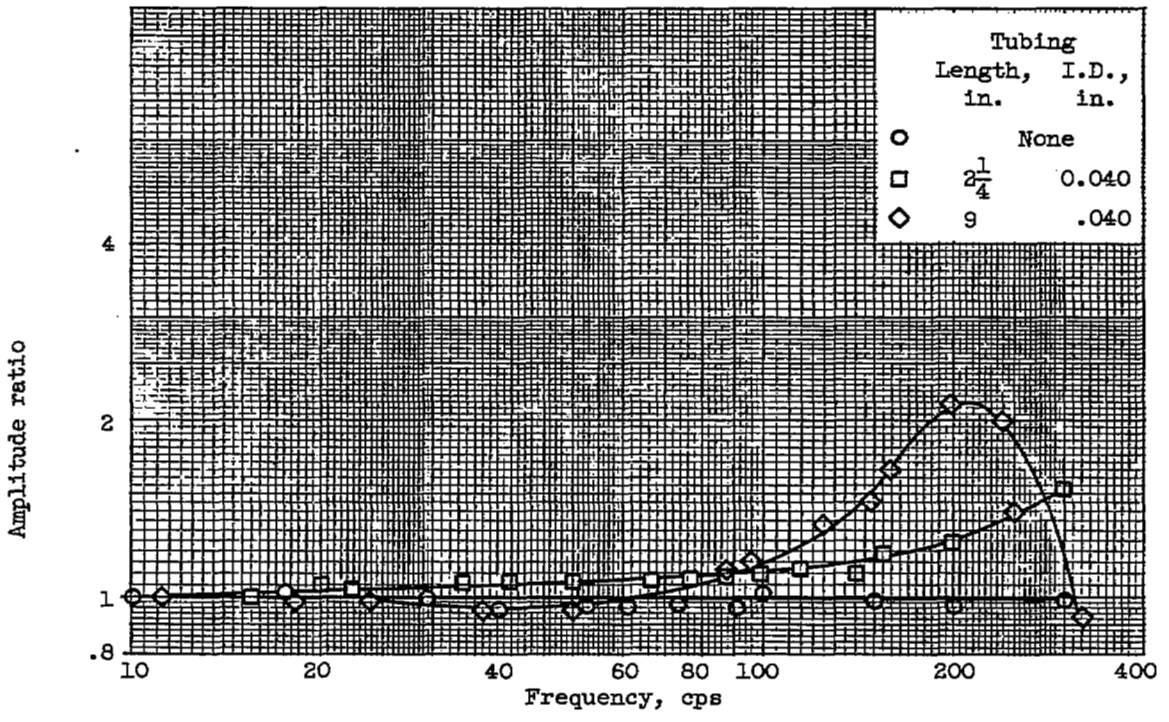

(a) Amplitude ratio of output to input.

Figure 6. - Frequency response of gas-pressure transducers.

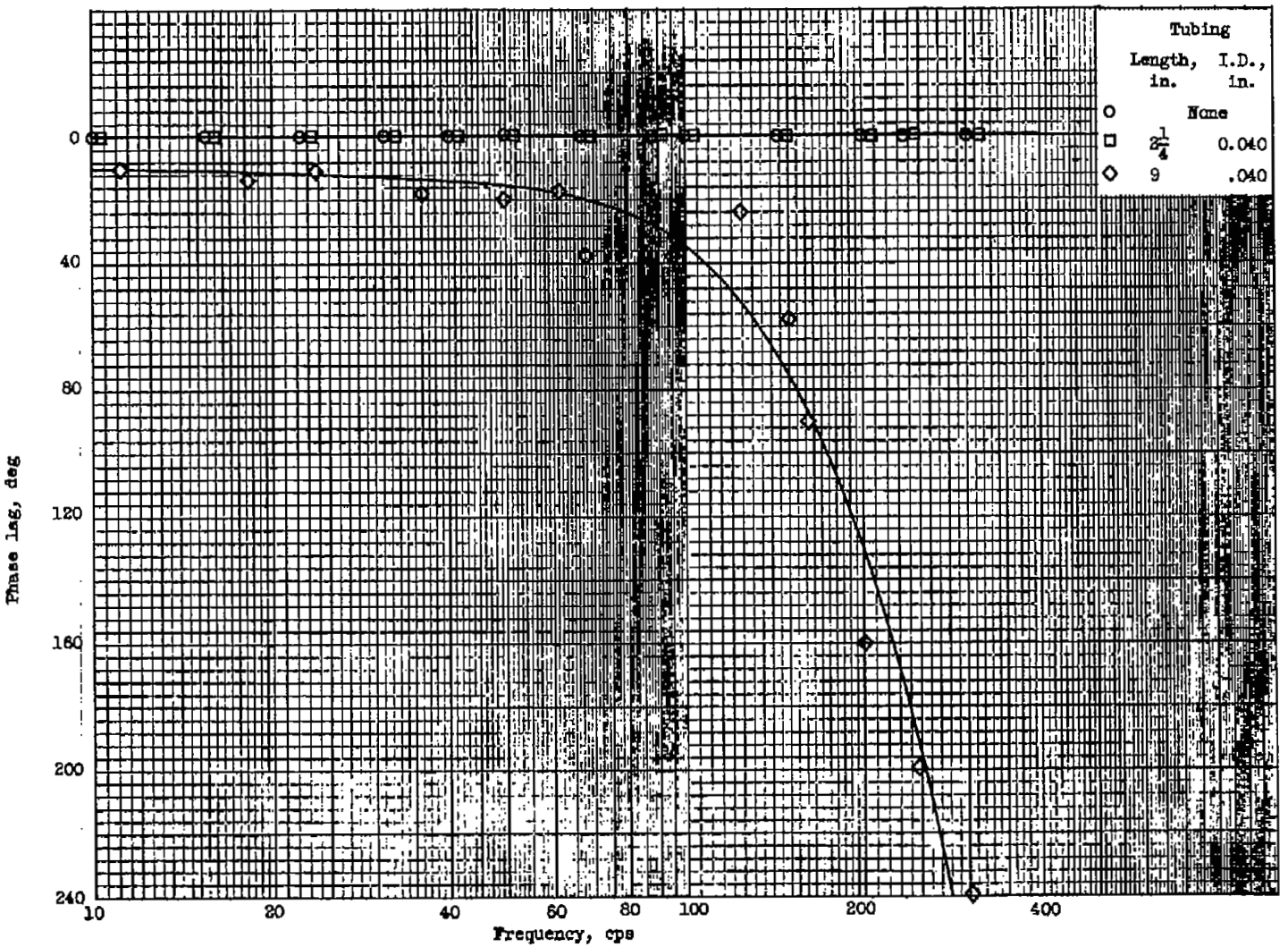

(b) Phase lag of output to input.

Figure 6. - Concluded. Frequency response of gas-pressure transducers.

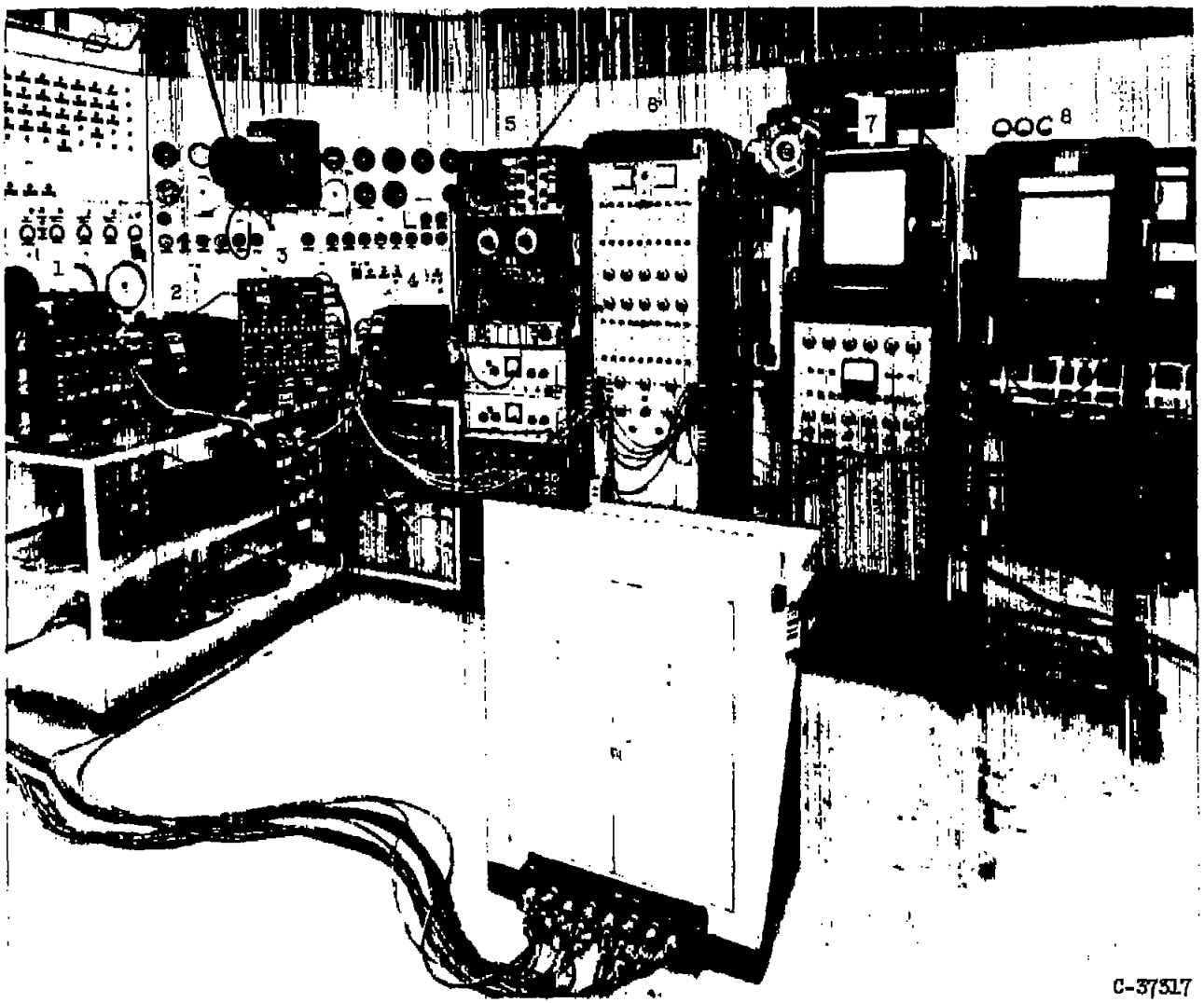

Figure 7. - Amplifiers and recording equipment.

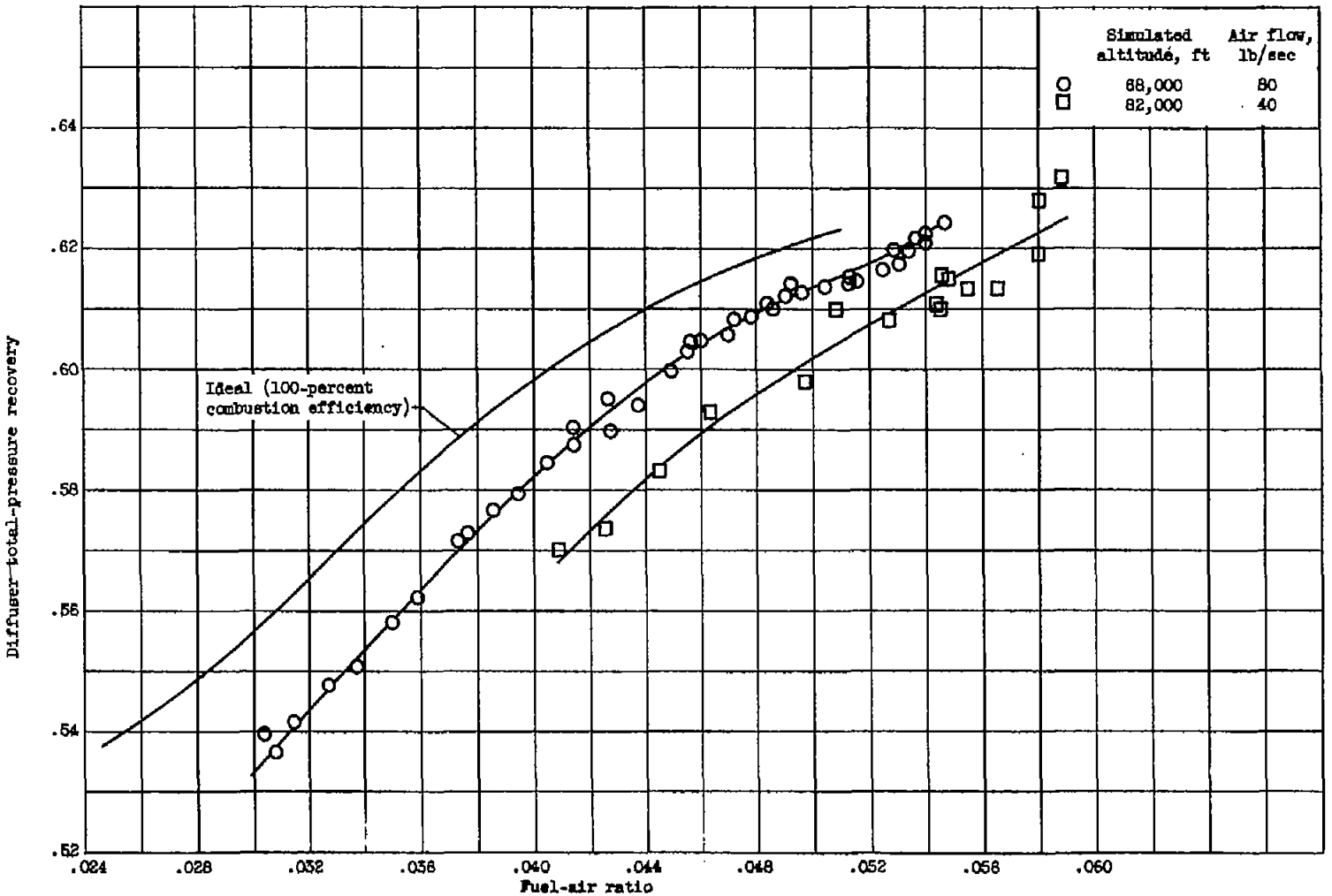

Figure 8. - Variation of diffuser recovery with fuel-air ratio.

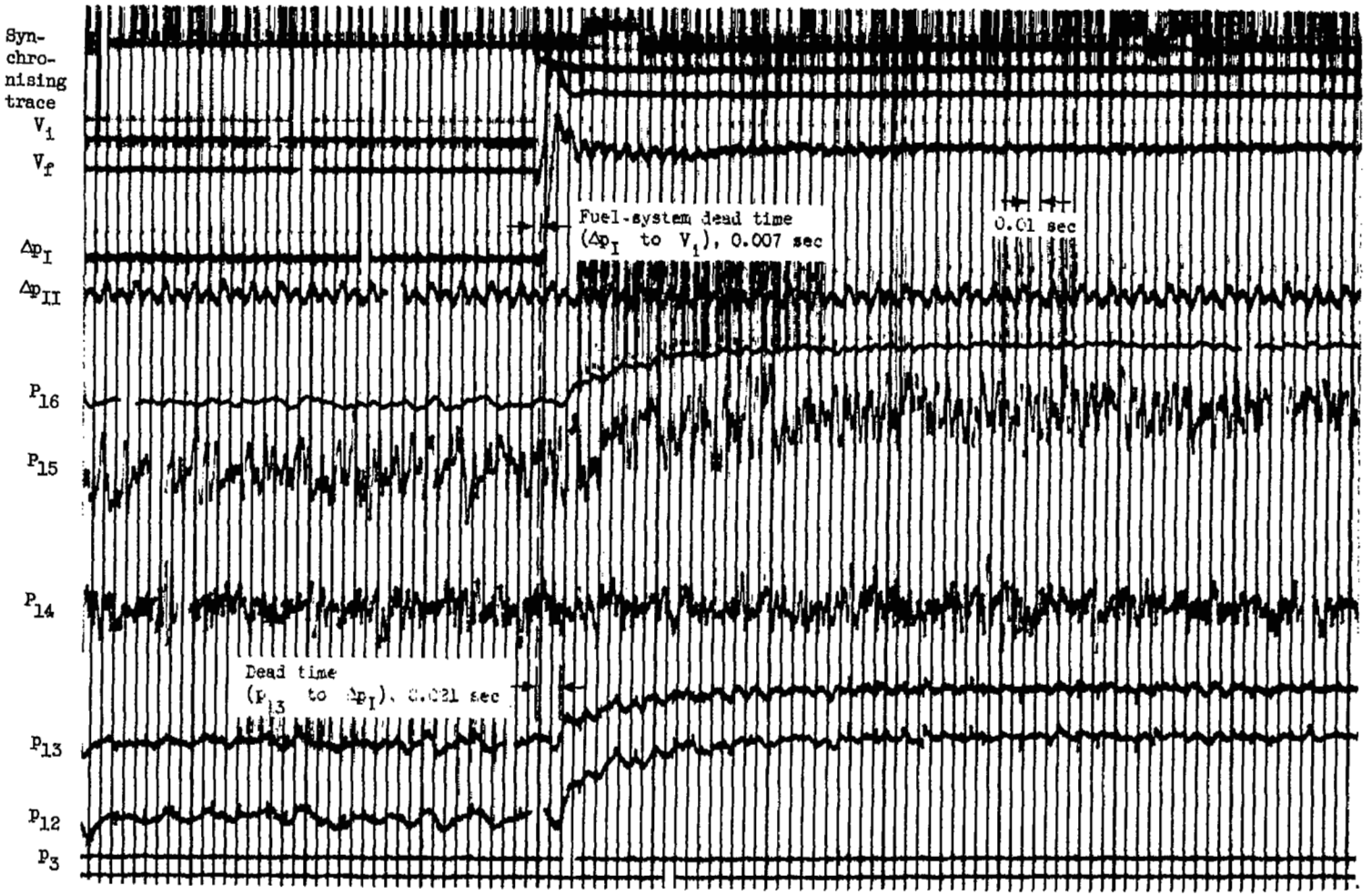

Figure 9. - Typical response to step increase in fuel flow. Initial diffuser total-pressure recovery, 0.553; final diffuser total-pressure recovery, 0.613; fuel-flow step, 0.738 pound per second; simulated altitude, 82,000 feet.

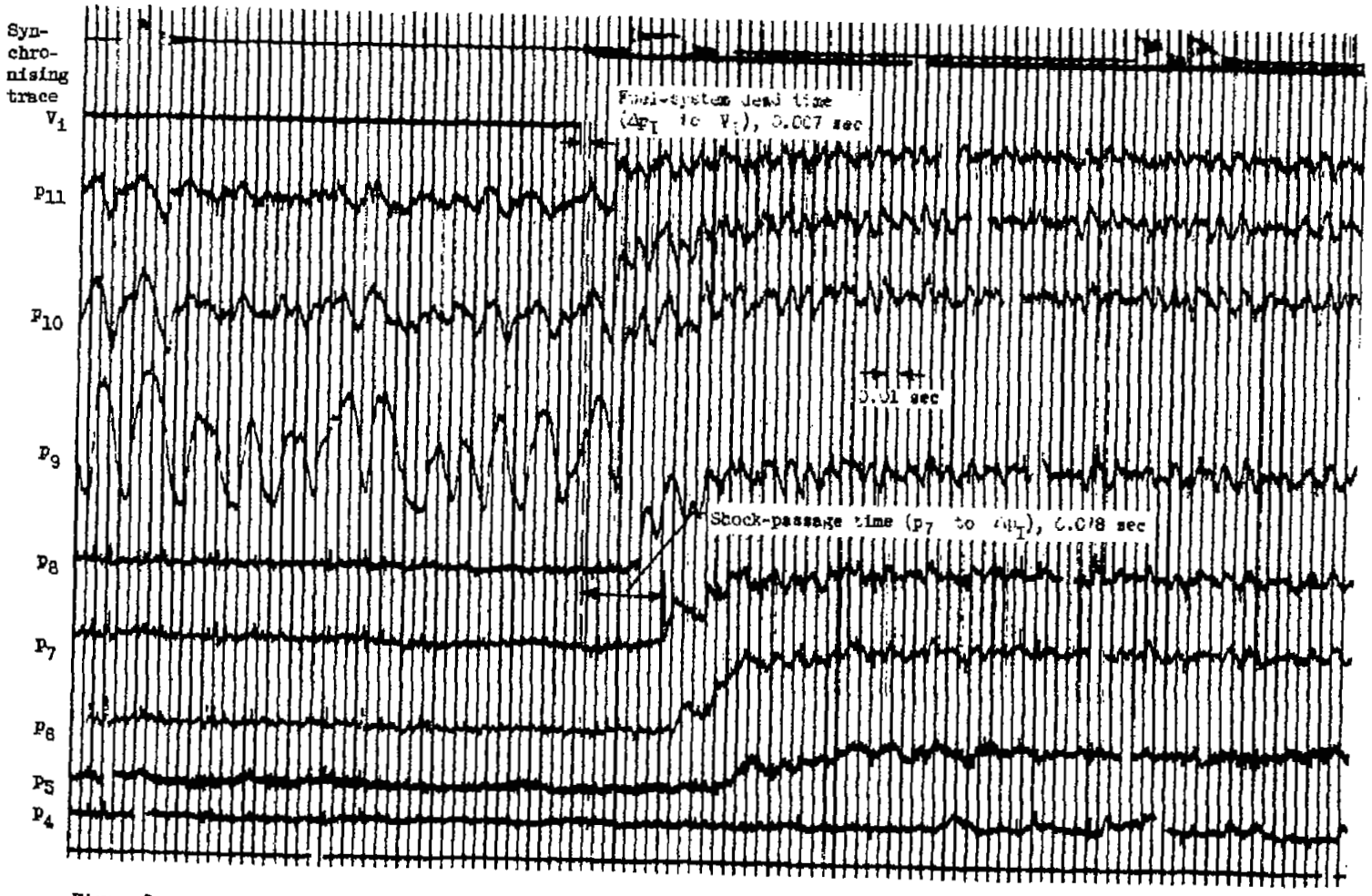

Figure 9. - Concluded. Typical response to step increase in fuel flow. Initial diffuser total-pressure recovery, 0.553; final diffuser total-pressure recovery, 0.615; fuel-flow step, 0.738 pound per second; simulated altitude, 82,000 feet.

Figure 10. - Typical response to step decrease in fuel flow. Initial diffuser total-pressure recovery, 0.613; final diffuser total-pressure recovery, 0.553; fuel-flow step, 0.738 pound per second; simulated altitude, 82,000 feet.

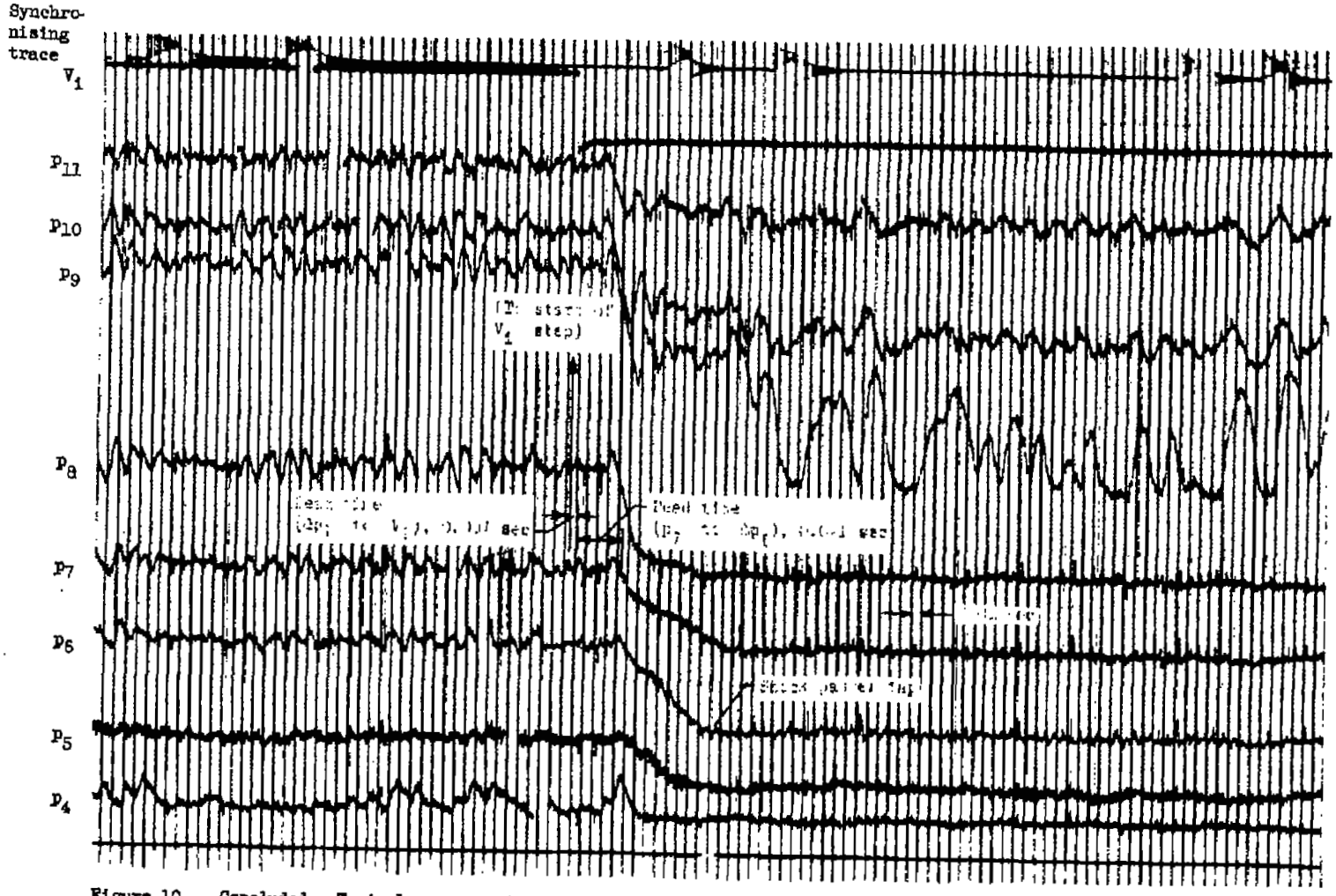

Figure 10. - Concluded. Typical response to step decrease in fuel flow. Initial diffuser total-pressure recovery, 0.613; final diffuser total-pressure recovery, 0.553; fuel-flow step, 0.738 pound per second; simulated altitude, 82,000 feet.

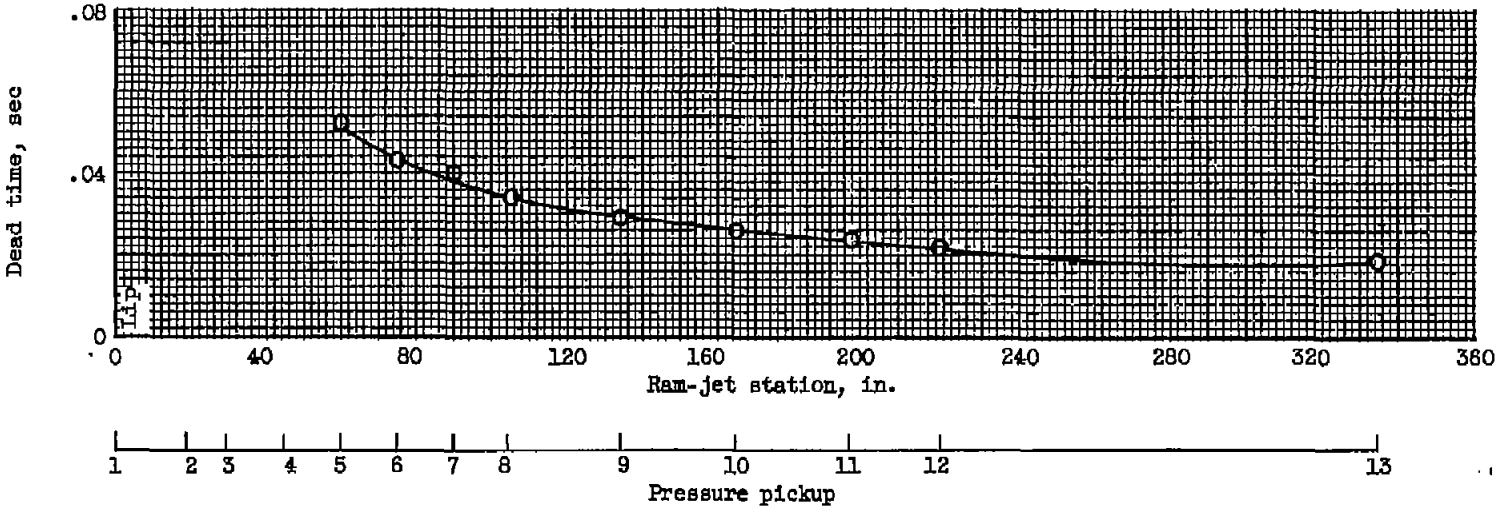

Figure 11. - Variation of dead time with ram-jet station. Initial diffuser total-pressure recovery, 0.616; step decrease in fuel flow, 0.246 pound per second; simulated altitude, 82,000 feet.

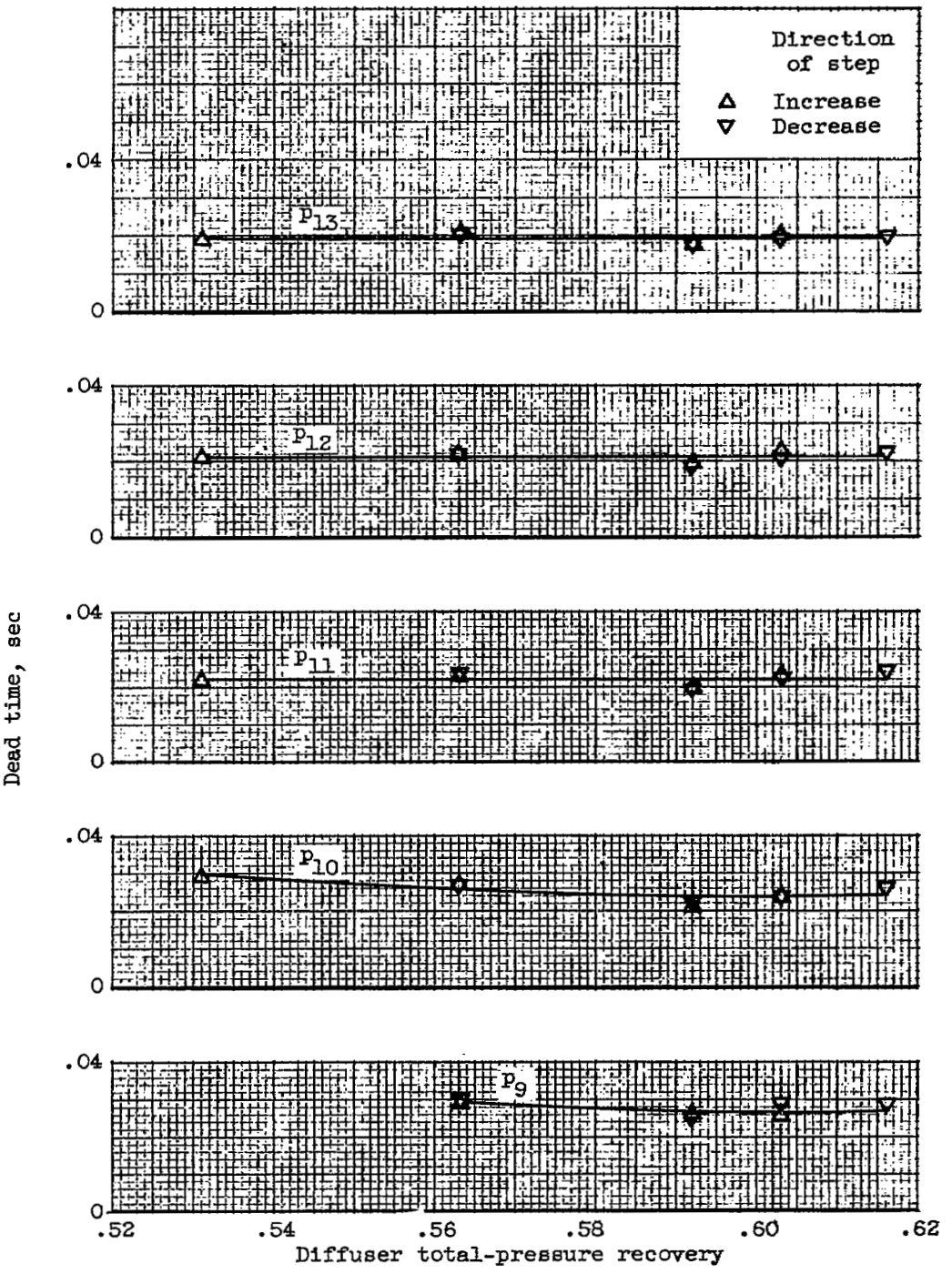

Figure 12. - Effect of diffuser total-pressure recovery and direction of fuel-flow step on dead time. Fuel-flow step, 0.246 pound per second; simulated altitude, 82,000 feet.

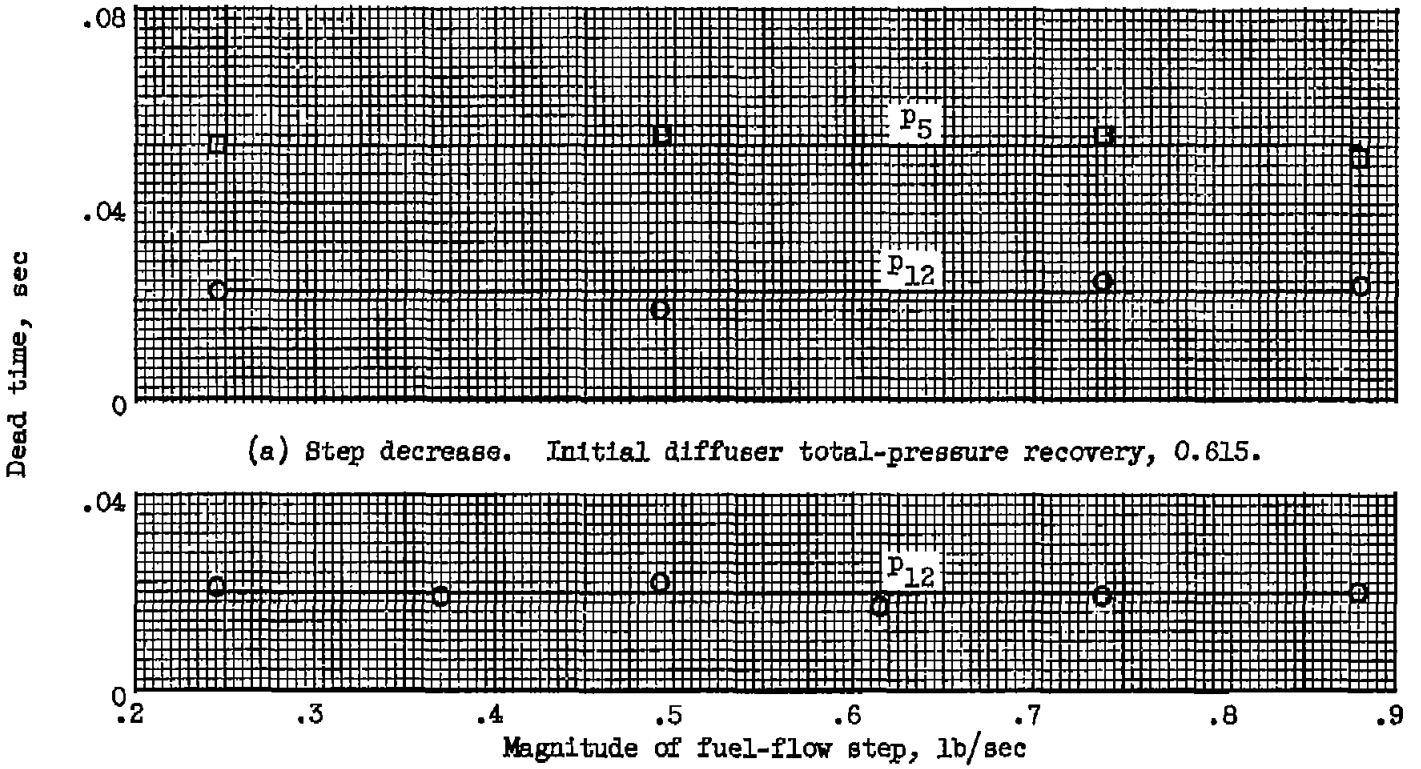

Figure 13. - Effect of magnitude of fuel-flow step on dead time. Simulated altitude, 82,000 feet.

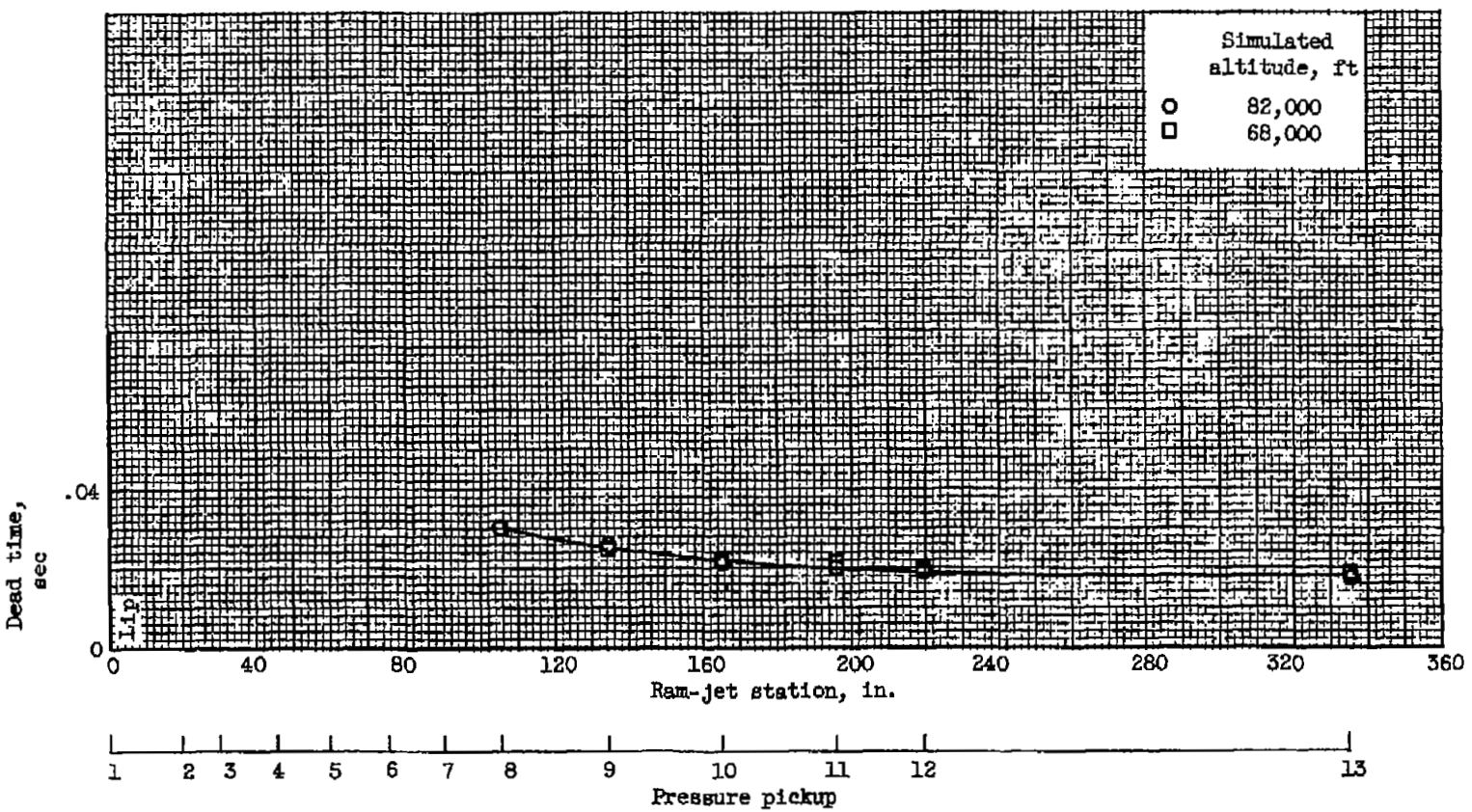

Figure 14. - Effect of altitude on dead time. Initial diffuser total-pressure recovery, 0.592; step increase in fuel flow, 0.006(fuel-air ratio).

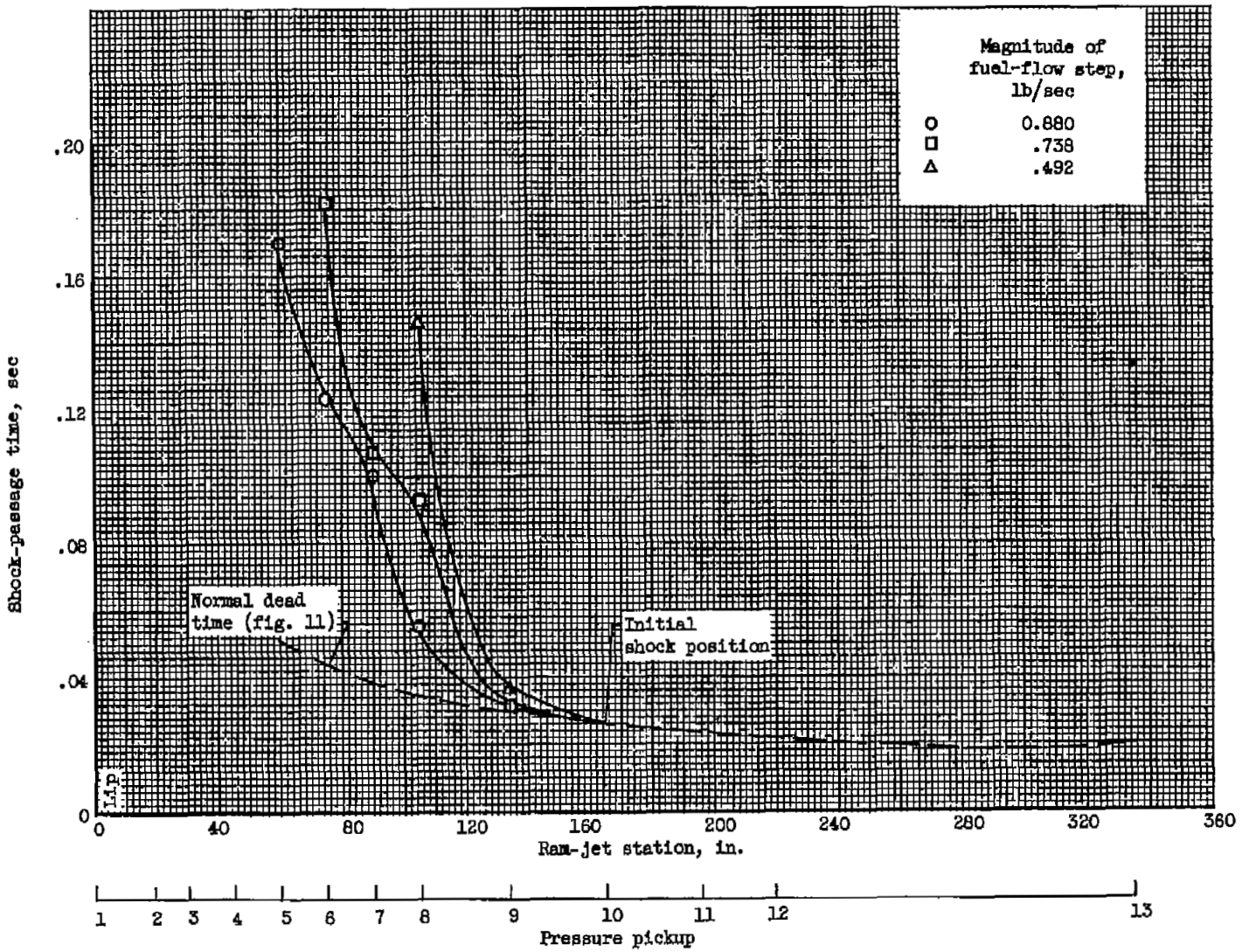

Figure 15. - Shock-passage times following step increases in fuel flow of various magnitudes. Initial diffuser total-pressure recovery, 0.530; simulated altitude, 82,000 feet.

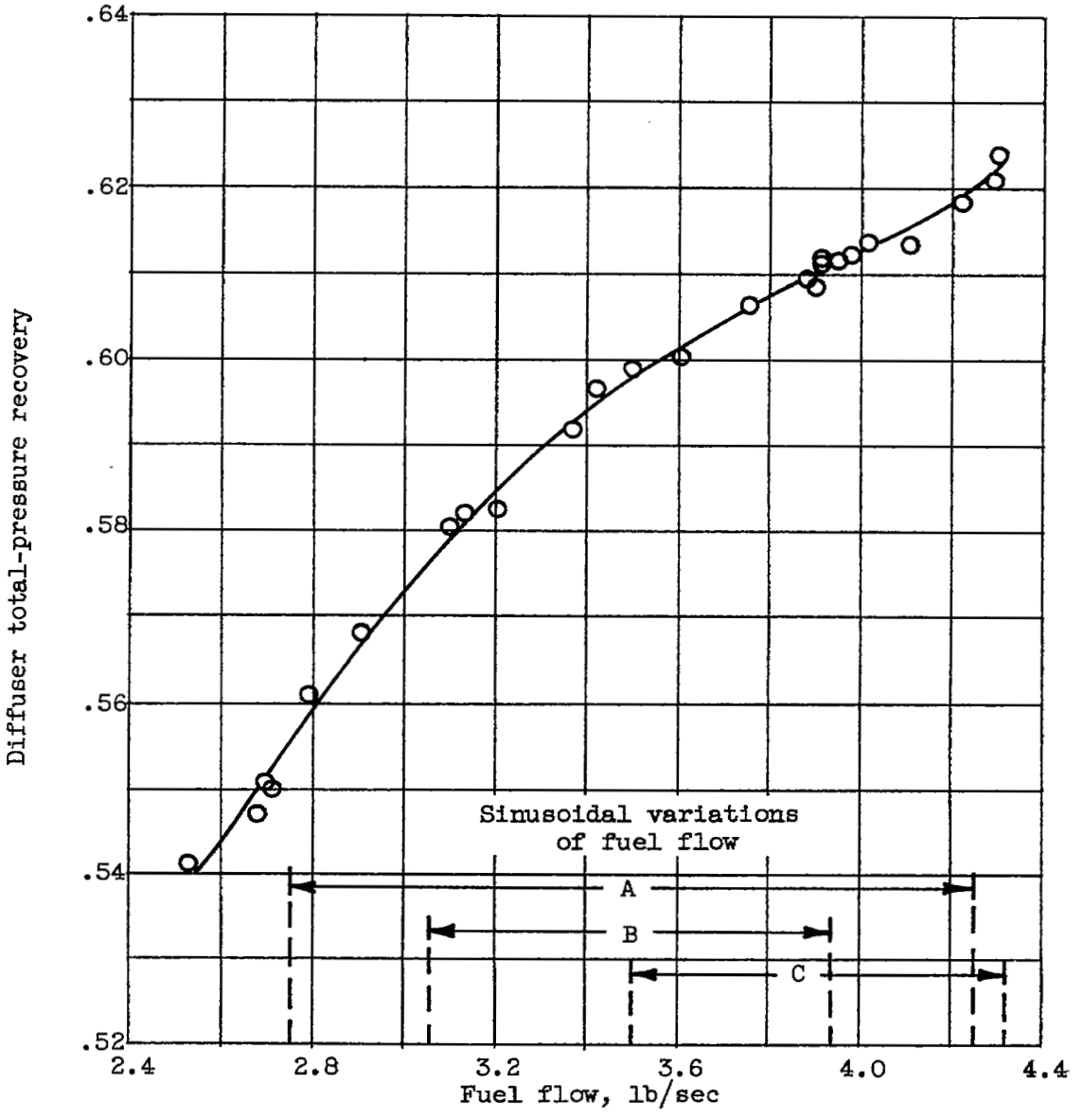

(a) Diffuser operation.

Figure 16. - Static characteristics of engine for fuel-flow range of frequency-response tests. Simulated altitude, 68,000 feet.

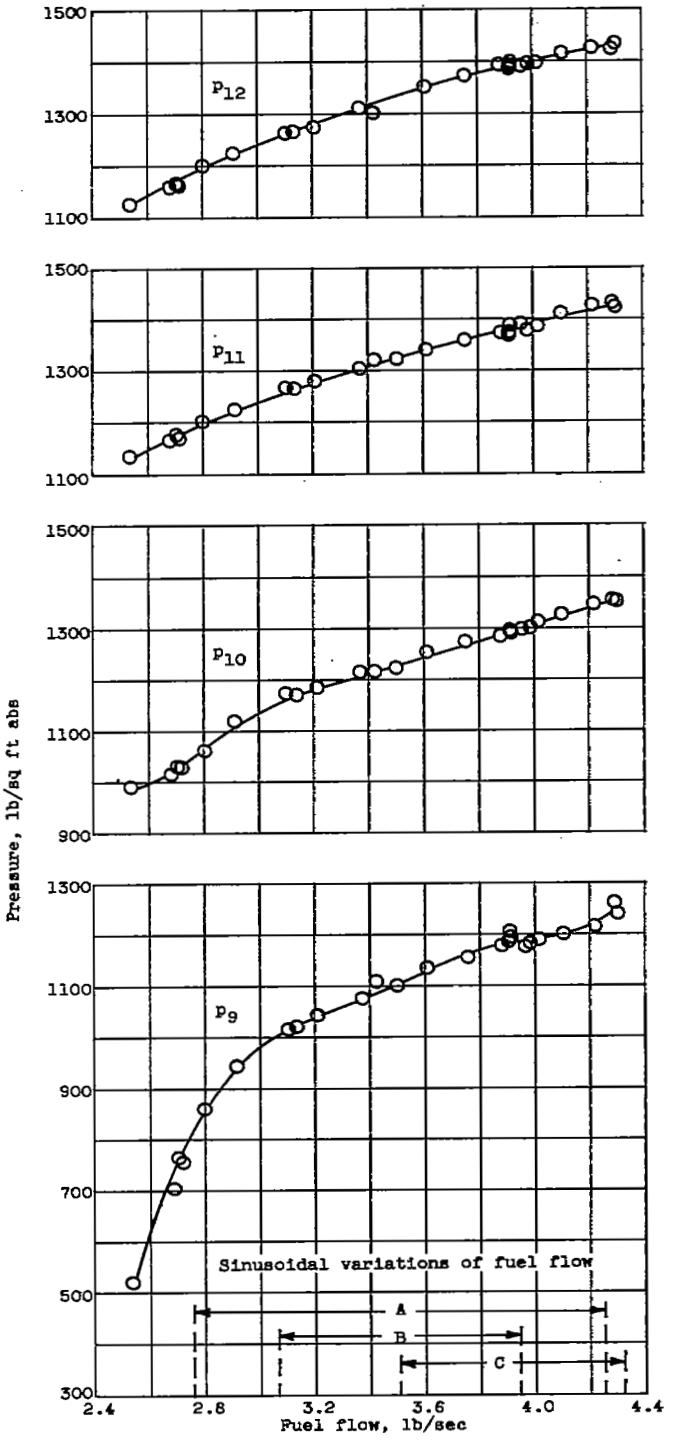

(b) Static pressures.

Figure 16. - Continued. Static characteristics of engine for fuel-flow range of frequency-response tests. Simulated altitude, 68,000 feet.

[redacted]

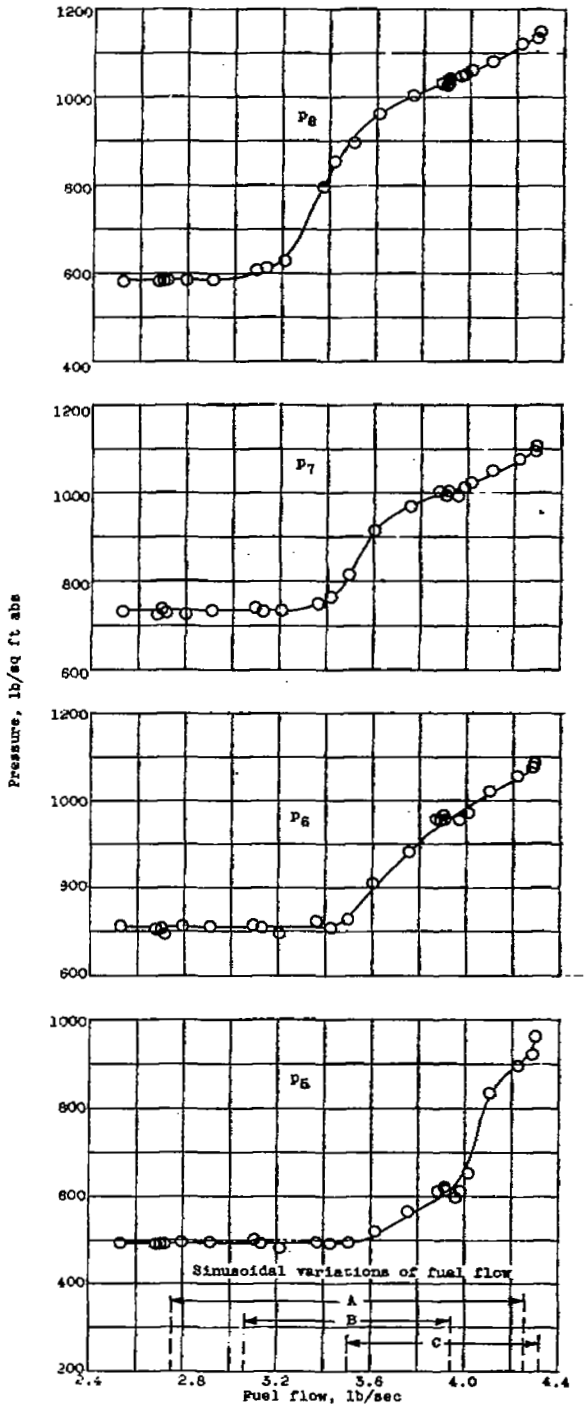

(b) Concluded. Static pressures.

Figure 16. - Continued. Static characteristics of engine for fuel-flow range of frequency-response tests. Simulated altitude, 68,000 feet.

[redacted]

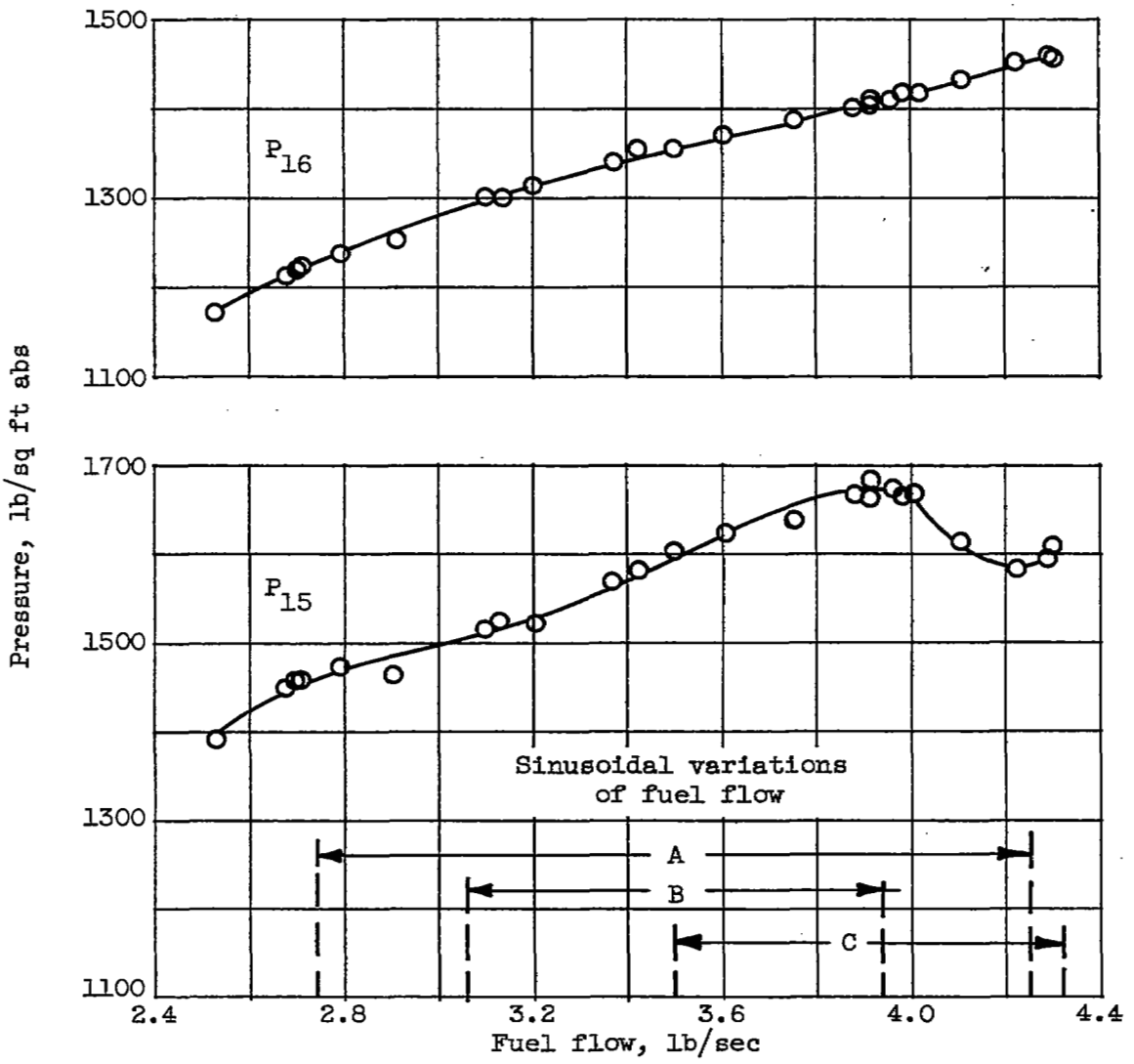

(c) Total pressures.

Figure 16. - Concluded. Static characteristics of engine for fuel-flow range of frequency-response tests. Simulated altitude, 68,000 feet.

[redacted]

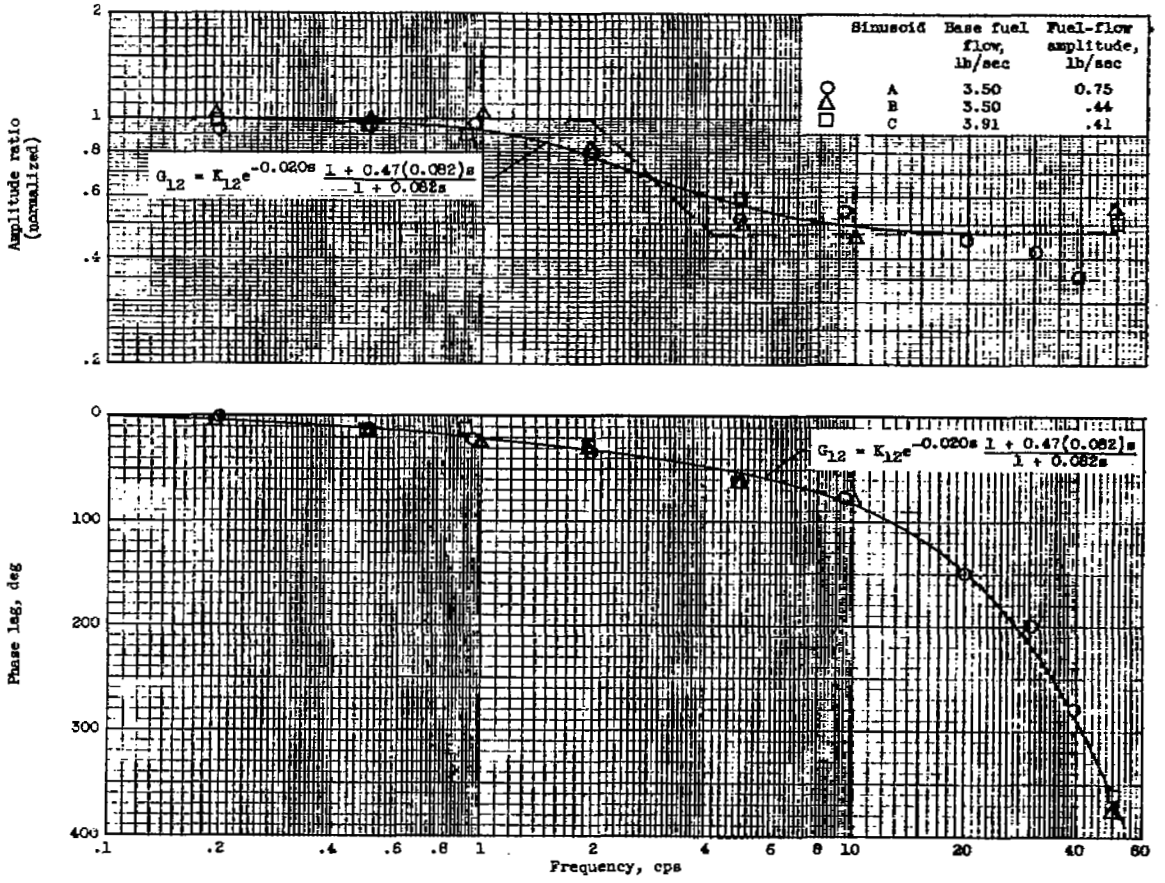

(a) Static pressure p_{12}.

Figure 17. - Frequency response of static pressures at stations downstream of shock during all three sinusoids. Altitude, 68,000 feet.

[redacted]

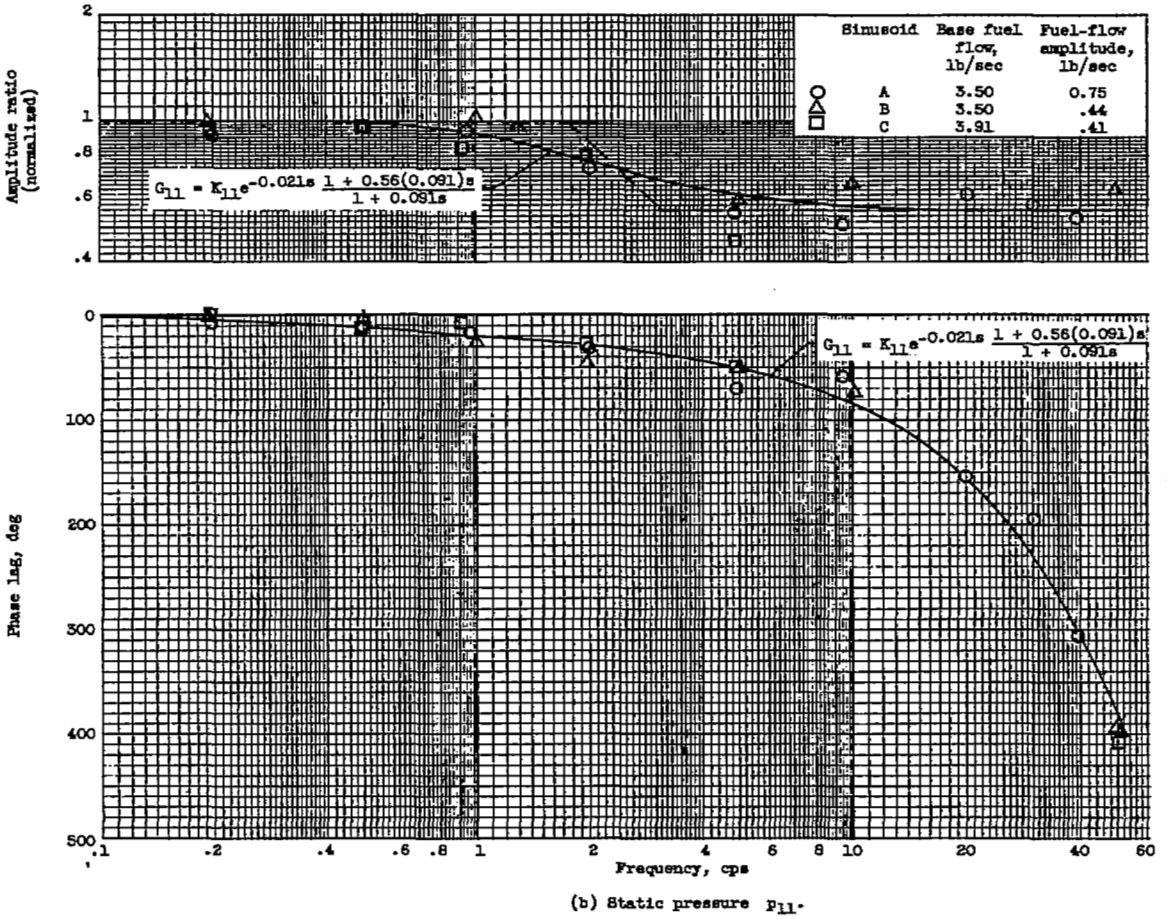

(b) Static pressure p_{11}.

Figure 17. - Continued. Frequency response of static pressures at stations downstream of shock during all three sinusoids. Altitude, 68,000 feet.

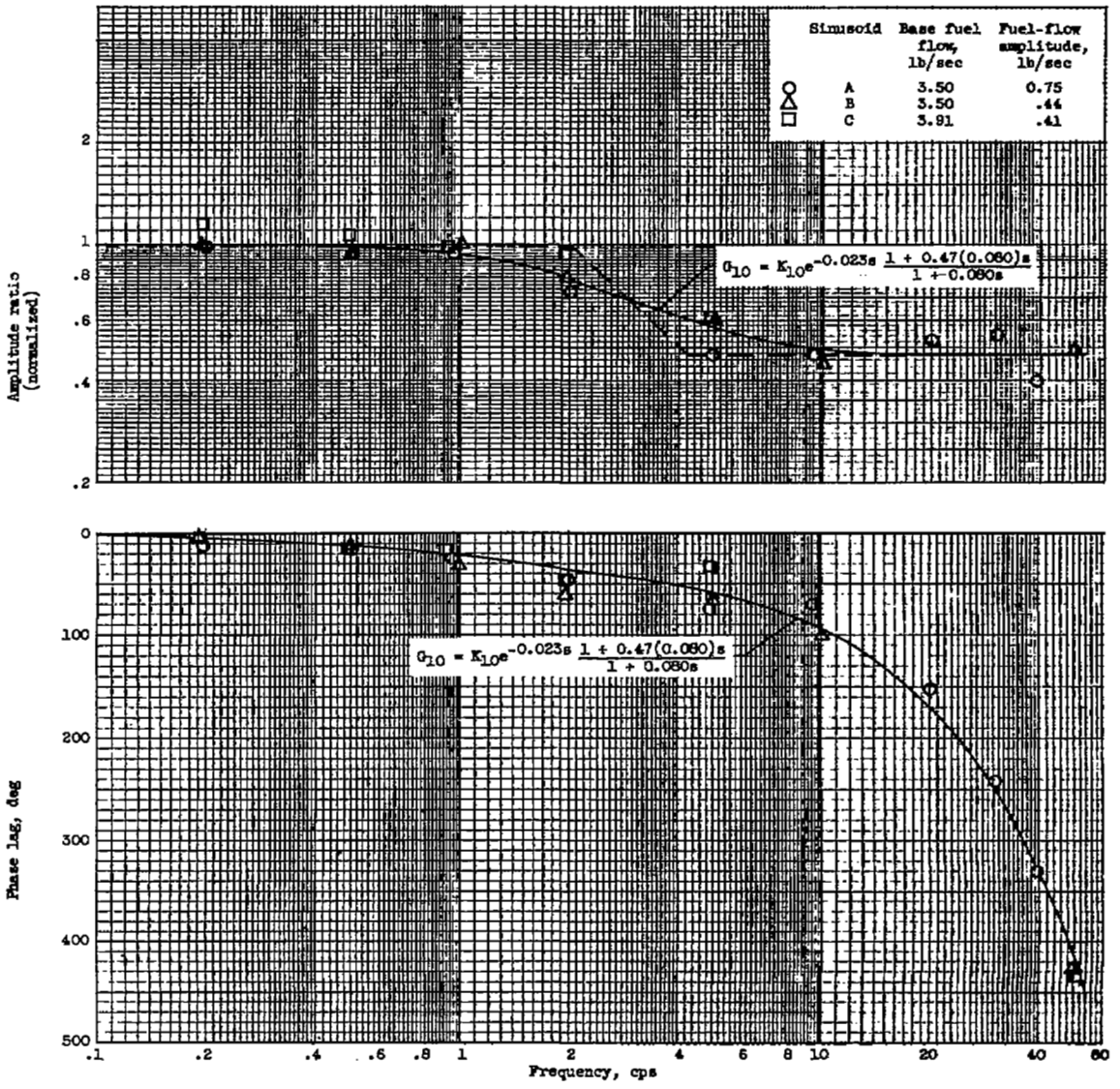

(c) Static pressure p_{10}.

Figure 17. - Continued. Frequency response of static pressures at stations downstream of shock during all three sinusoids. Altitude, 68,000 feet.

[redacted]

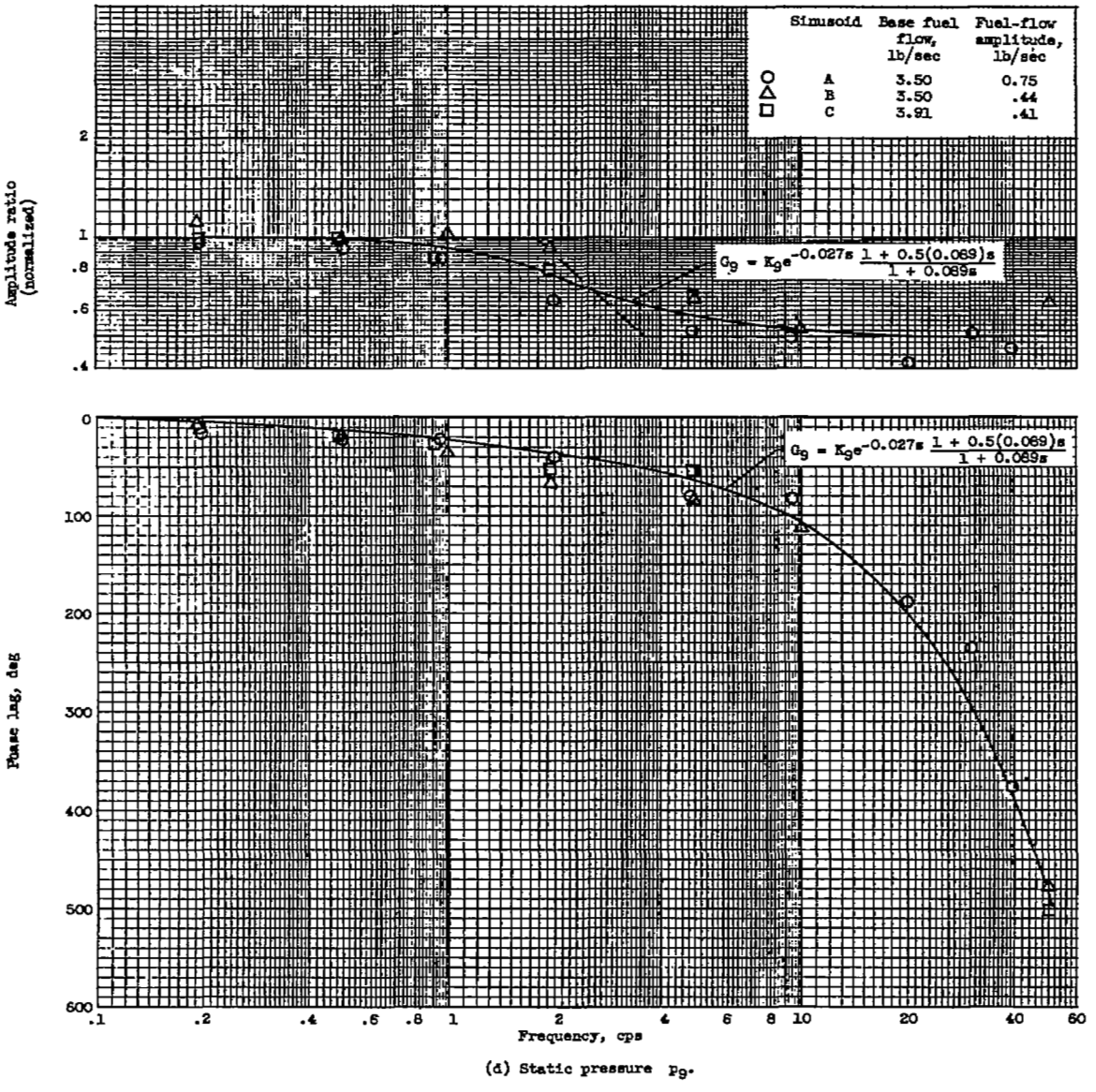

(d) Static pressure P_g.

Figure 17. - Concluded. Frequency response of static pressures at stations downstream of shock during all three sinusoids. Altitude, 68,000 feet.

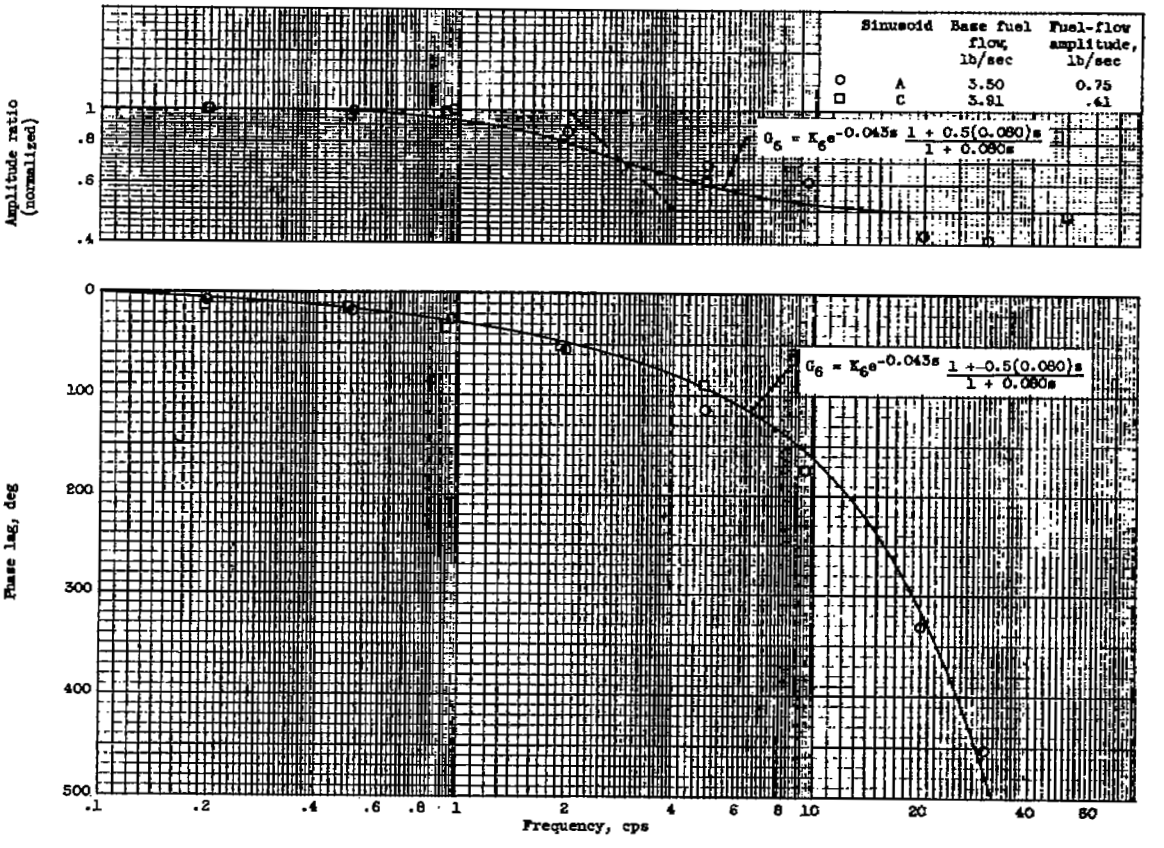

Figure 18. - Frequency response of static pressure p_6. Altitude, 68,000 feet.

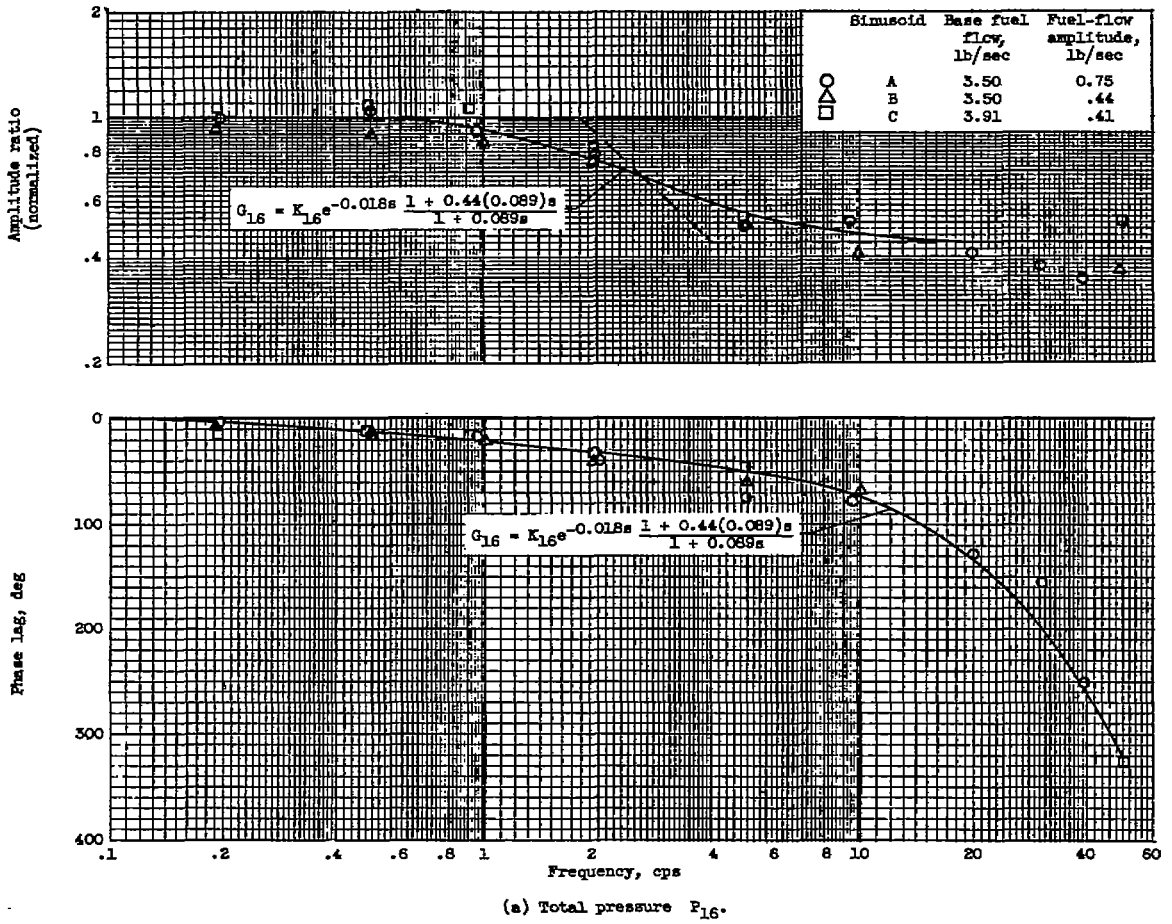

(a) Total pressure P_{16}.

Figure 19. - Frequency response of total pressures. Altitude, 68,000 feet.

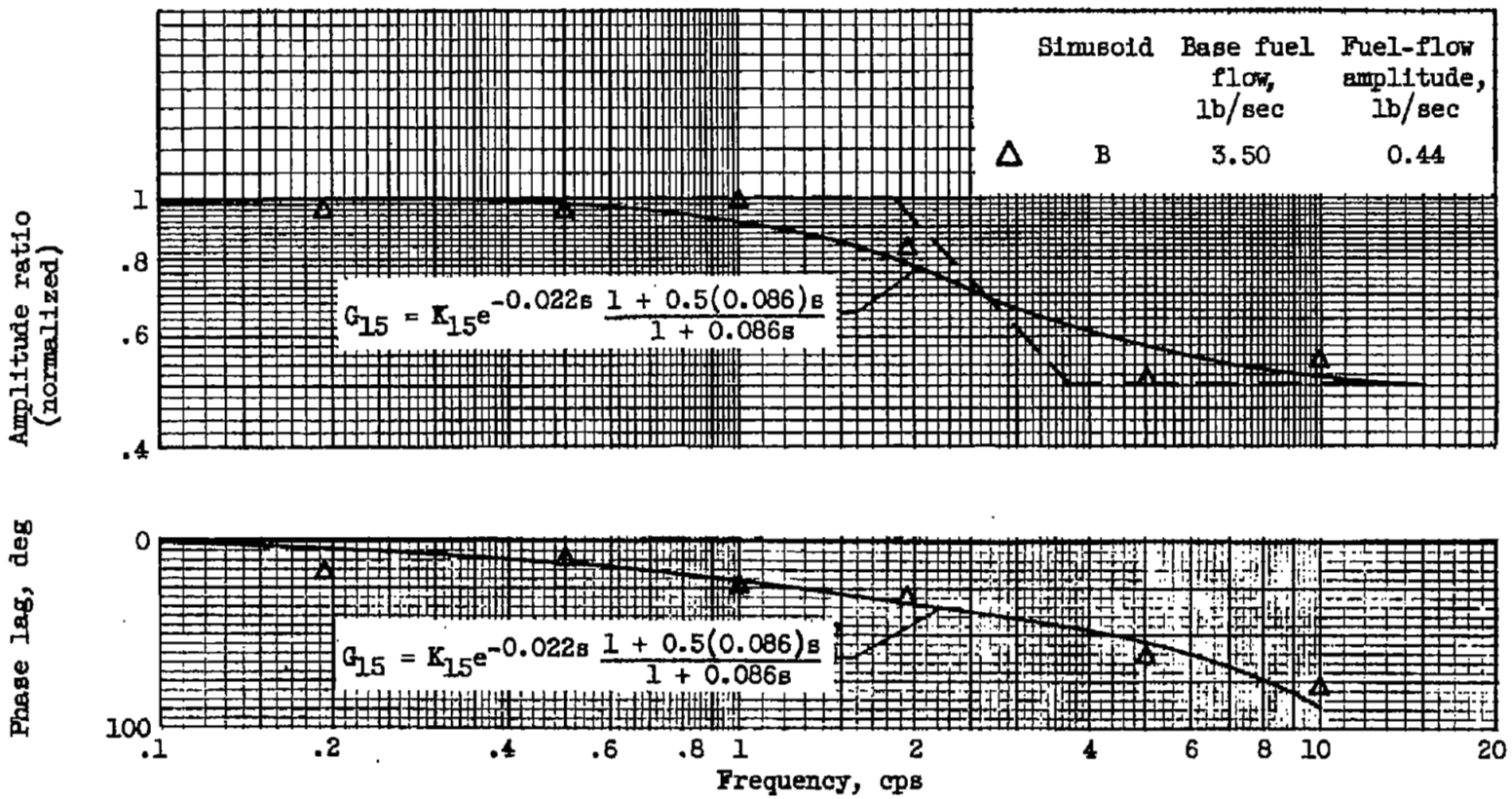

(b) Total pressure P_{15}.

Figure 19. - Concluded. Frequency response of total pressures. Altitude, 68,000 feet.

NACA - Langley Field, Va.